ABSTRACT

Title of Thesis:	VENTILATION IMPACT ON AIRBORNE TRANSMISSION OF RESPIRATORY ILLNESS IN STUDENT DORMITORIES
	Sara Taylor Jenkins, Master of Science, 2018
Thesis Directed By:	Dr. Jelena Srebric, Professor of Mechanical Engineering

This work presents a study of the effect of ventilation rates on the bioaerosols that cause upper respiratory illness. A network of 147 sensors was placed in a pair of dormitories on a college campus to measure carbon dioxide concentrations over two semesters. The concentration results served as input into multi-zone ventilation models of the two buildings, which had different heating, ventilation, and air conditioning (HVAC) systems. The dormitory with a central mechanical ventilation system had, as expected, a higher turnover of fresh air compared to the other, which relied on exhaust fans and infiltration. This well-ventilated building also contained far fewer occupants with recorded upper respiratory illness incidence in comparison to the poorly ventilated building. The central ventilation system increased dorm room ventilation rates by 500%, while decreasing respiratory illness incidence by over 85%. Comparative studies have shown similar findings with increased ventilation reducing incidence of upper respiratory illness by an order of magnitude.

VENTILATION IMPACT ON AIRBORNE TRANSMISSION OF RESPIRATORY ILLNESS IN STUDENT DORMITORIES

by

Sara Taylor Jenkins

Thesis submitted to the Faculty of the Graduate School of the
University of Maryland, College Park, in partial fulfillment
of the requirements for the degree of
Master of Science
2018

Advisory Committee:
Professor Jelena Srebric, Chair
Professor Peter Chung
Professor Amr Baz

Dedication

To my family.

Acknowledgements

First, I would like to thank my advisor, Dr. Jelena Srebric, whose constant support, advice, and incredible technical expertise helped me to do what I didn't think I could.

Second, the other members of my defense committee, Dr. Amr Baz and Dr. Peter Chung, for helping me to finish my paper in time and for being terrific teachers during my time at the University of Maryland.

Third, I want to thank my friends in the lab, including Kofi Addo, whose positivity and good nature made even the most menial tasks enjoyable, and Joshua Ehizibolo, whose commitment was absolutely inspiring. Sebastian, for creating the CONTAM models that made this whole study possible. Mohammad Nomeli, for his great advice, and Tanishq Agarwala, for his brilliant MATLAB codes. Daniel Dalgo, Nicholas Mattise, Harshil Nagda, and everyone else, for offering help whenever and wherever they could.

Lastly, and most importantly, I have to thank my family and friends, who made me the person I am today, and also helped me find and fix last minute grammar errors. Mom and Dad, you remain the best last minute proof readers a daughter could ask for, and Marissa, thanks for you constant efforts to keep me sane throughout the whole last semester.

Table of Contents

List of Tables

List of Figures

List of Abbreviations

ACH	Air changes per hour
AHU	Air handling unit
ARI	Acute respiratory illness
ASHRAE	American Society of Heating, Refrigerating and Air-Conditioning Engineers
CATCH	Characterizing and Tracking College Health
CFD	Computational fluid dynamics
Cfm	Cubic feet per minute
Cfu	Colony-forming units
CO_2	Carbon dioxide
DARPA	Defense Advanced Research Projects Agency
DOAS	Dedicated outdoor air system
FCU	Fan coil unit
HVAC	Heating, ventilation, and air conditioning
HVB	High Ventilation Building
LVB	Low Ventilation Building
qRT-PCR	Quantitative reverse transcription polymerase chain reaction

Nomenclature

C_{CO2} or C_{virus}	Concentration of contaminant
C_D	Discharge coefficient
$\dot{N}$	Contaminant source flow rate
n	Flow exponent
ΔP	Change in pressure
$\dot{V}$	Volumetric flow rate

Chapter 1: Introduction

1.1: Purpose

This study was conducted to contribute to findings that link poor ventilation to increases in illness caused by airborne contaminants. Two buildings, one with a newly installed, state-of-the-art central ventilation system and the other relying on infiltration and exhaust fans for outdoor air exchange, were monitored for eight months. The sensors placed in each building recorded carbon dioxide (CO_2) concentrations in various rooms and hallways. Models of the contrasting buildings were created in CONTAM to help calculate the ventilation rates. A record of incidences of acute respiratory illness (ARI), detected using quantitative reverse transcription polymerase chain reaction (qRT-PCR) tests, was kept and compared to ventilation rates and CO_2 concentrations in these rooms of interest.

Three study aims motivate this thesis:

1. Collect and calibrate environmental data for an array of rooms in two dormitories.
2. Create multizone models for the two dormitories and use them to calculate accurate ventilation rates in the two buildings under a variety of conditions.
3. Determine if there is an association between low ventilation rates and increased ARI occurrences.

In addition to these goals, the aforementioned models were used to predict locations of increased virus exposure based on the locations of the source rooms and flow rates between adjacent rooms.

Going further, an energy analysis will be performed on the two buildings to evaluate the costs of the building renovation. The overarching goal of this study is to determine the most cost and energy efficient way to improve overall building ventilation, which in turn will improve student health and proficiency. Further research will also eventually incorporate UV irradiation of contaminated air to destroy viral RNA, which lowers the probability of infection by decreasing the concentration of potent airborne viruses that cause respiratory illness.

1.2: Overview of Different Heating, Ventilation, and Air Conditioning Systems

Indoor air conditioning is accomplished in two ways, by heating or cooling the air already inside the building or by pumping in outside air and treating the air before distributing it into the building. The latter method simultaneously improves ventilation by moving air in and out of a room while modifying its temperature. This study focuses on two dormitories, denoted as high and low ventilation buildings based on the heating, ventilation, and air conditioning (HVAC) system installed. Relevant components of the observed systems are described below.

1.2.1 Fan Coil Units

Fan coil units, or FCUs, are heating/cooling boxes that operate independently of each other. They are commonly used as residential or commercial air conditioners. The FCU draws in air from the room. The air is run through rows of coils filled with a liquid or gas coolant, and then pumped back out into the room. The air passing through is heated or cooled to modify temperatures to those set by the system controls.

While an FCU can modify temperature, there is no net change in air flow in or out of a room, as internal air is simply circulated through the unit. They are often paired with air handling units (AHUs) that introduce air from outside the building (Chu, Jong, & Huang, 2005) (Ke, Weng, & Chiang, 2007).

1.2.2 Dedicated Outdoor Air Systems

Dedicated outdoor air systems, or DOAS, are a form of central HVAC system that pump in outside air, add or subtract heat, and then introduce the air into the building. It uses AHUs to bring fresh air to every floor of the building, with ventilation shafts bringing air into individual rooms. Exhausts are also placed around the building to extract the old air and pump it back out.

DOAS delivers air to individual zones of a building, rather than transferring it from room to room via infiltration. Treatment of this air is conducted separately from the treatment of internal air, which is treated by FCUs or other temperature and humidity controls that work well alongside DOAS. Both of these methodologies have the dual advantage of increasing energy saving potential in the building as well (Dieckmann, Roth, & Brodrick, 2003). Figure 1 shows a layout of a simple DOAS system, especially the zone delivery and incorporation of outside air.

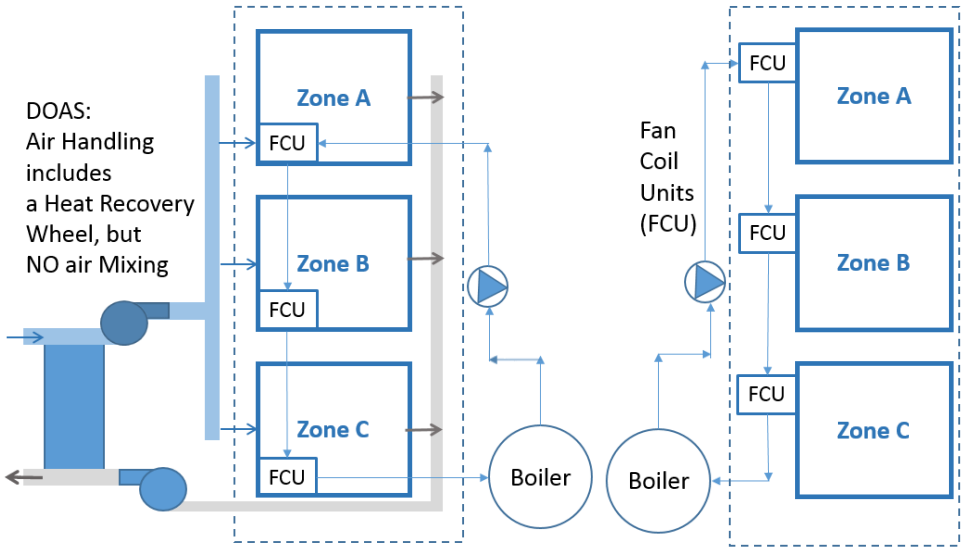

Figure 1: DOAS in high ventilation dormitory (left) and local fan coil units in low ventilation dormitory (right) (Group, 2016)

1.2.3 Studied Dormitories

Two dormitories, similar in age, construction, and maintenance, were chosen to represent different ventilation qualities. The buildings sit adjacent to one another on the north end of the campus, as shown in Figure 2.

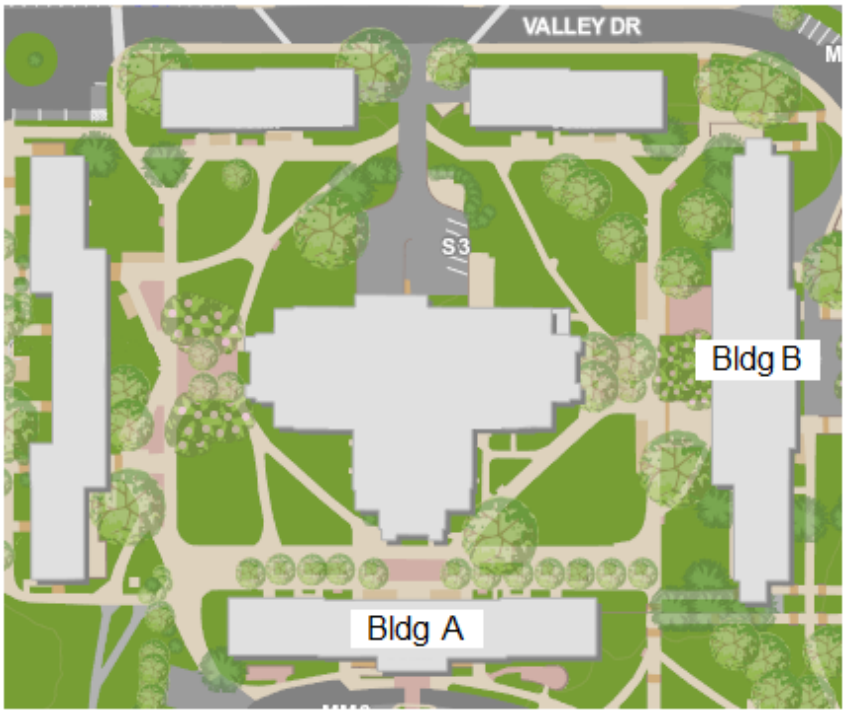

Figure 2: Building A and Building B on campus (Residence Halls: Cambridge Community, 2018)

Important to note is that the set point temperatures in the University of Maryland dormitories are 74 in the summer and 70 in the winter, in accordance to the university's campus energy standards (Residence Halls: Cambridge Community, 2018).

Building A is the study's high ventilation building (HVB). It was constructed in 1962, but underwent renovation in 2015, when a DOAS was installed to provide fresh air to nearly all of the rooms in the building. This dormitory, neighbor to Building B, rises 4 stories high and has a capacity of 223 co-ed students (Residence Halls: Cambridge Community, 2018). Every student room has an FCU and an inlet for the DOAS to pump in outside air. Bathrooms and study lounges have exhaust air returns, driven by the single AHU's exhaust fan. The same AHU provides every one of the student's rooms with 22-29 cfm of fresh air as part of the DOAS and central ventilation

system, while study lounges receive 85 cfm and bathrooms anywhere from 150 to 300 cfm, depending on size.

Building B, the low ventilation building (LVB), was also constructed in 1962. The 7-story, co-ed dormitory has a capacity of 545 students (Residence Halls: Cambridge Community, 2018). It is set up with FCUs in all of the student rooms and two heating zones, in the east and west wings of the building. Specific individual rooms including bathrooms on every floor and study lounges on the first two floors have exhaust air returns, driven by four exhaust fans. The basement and first floor also have four AHUs. The two basement AHUs have design airflows of 4000 and 8000 cubic feet per minute (cfm), the two on the first floor have design airflows of 5000 cfm each.

1.3: Indoor Microbiome

Built spaces, in their attempt to manipulate nature to make it more habitable for human life, create niches apart from the outside world. An indoor living space has its own temperature, light, humidity, depending on the allowances made by those who built it. The flow of air through and around the structure can be altered, whether four solid walls create a stagnant space, or a complex ventilation system pumps in outside air to renew the indoor gases. Improper ventilation facilitates the growth of an unhealthy indoor microbiome, especially as the time the residents spend in the space or the number of residents in the space increases. The residents act as sources of contaminant inside the rooms, exhaling viruses and bacteria that can remain in the air for a long period of time if not circulated out by an active ventilation system. Viruses especially, due to their small size, referred to in this context as their aerodynamic equivalent diameter (AED), have a long settling time. The possibility of another

roommate or passerby inhaling the virus increases with decreased AED (Hall, 2017) (McDevitt, et al., 2013).

The dominant mode of the spread of the influenza virus changes with the conditions in the room. It is not always airborne shedding or physical surface-to-skin or skin-to-skin contact (Hall, 2017). The variability in particle sizes and dorm room conditions makes it difficult to predict the settling times of various airborne viruses and bacteria, but it can take minutes to days. Influenza virus clusters average 1μm – 3μm in diameter, and generally take 1-12 hours to settle five feet in still air (McDevitt, et al., 2013).

Students who participated in this study were tested for a variety of respiratory illness-causing viruses during the early spring semester, in the heart of flu season when students have the highest likelihood of falling ill. University of Maryland, like most colleges, offers a yearly flu shot to all of its students (Flu Vaccine Clinic Details, 2018), but not all participate and many are infected every winter. As of January 30th 2018, 4,500 students had obtained this year's shot from the University Health Clinic. This number dwarfs in comparison to the 40,500 total students enrolled at the University of Maryland, though some students might have obtained the shot from other proprietors.

The ARI occurrences of interest in this study are not the ones acquired outside of the dormitory. The ventilation system has little relevancy on those ARI cases, as it has no effect on illnesses the students pick up in other locations. The cases of interest were those that stemmed from the source case, defined as the resident who first reported a confirmed ARI. When a student falls ill and emits contaminants into the air, and those contaminants find their way to other dormitory residents rather than being purged from

the building by the ventilation system, it provides evidence towards the fallacies of the ventilation system. Dates and locations of reported ARIs were used to model the potential association between type of ventilation system and reported ARI in dormitory residents. For example, if a participant in room 1 tested positive for influenza B, and then a participant in room 2, next to room 1, contracted influenza B two days later, it would be highly probable that the second incidence was a result of the first, even if the original patient contracted the illness outside the hall. In these cases, the indoor microbiome has been allowed to flourish, increasing the likelihood of illnesses to spread from roommate to roommate and then room to room.

1.4 Literature Review

The primary goal of this thesis was to determine the ventilation rates in two dormitories, using CO_2 concentrations collected over four months to validate the models. Given the number of zones that were considered, a few critical simplifications had to be made to enable these calculations, nonetheless, the overall methodology stems from the work of previous studies on ventilation rate calculation.

Indoor air flow rate analyses have been performed before, in a variety of settings. These methods utilize the information about the tradeoff of air into and out of a space, along with the changes that occur inside of the room, to track the flow of the air mass as well as the particles carried with it. Methods have included computational fluid dynamics (CFD) simulations integrated with Eulerian steady state passive scalar models, Lagrangian particle tracking, and the Wells-Riley equation. The Eulerian method of fluid flow development takes a broad stroke approach compared to the Langrangian method. In general fluid dynamics, the velocity field is used to determine

particle path fields via integration paired with a set of boundary conditions that define the space. Combined with CFD, it is possible to compute the particle paths across an entire space. Using the Eulerian method, the scalar is attached to a transport equation to determine the mass fraction of active to deactivated microorganisms (Pichurov, et al., 2015). The Lagrangian method uses a discrete phase model to predict the movement of particles. Based on their location through many time steps, it is possible to determine what percent will spend sufficient time in the UV region, and the probability of their being deactivated can be calculated (Pichurov, et al., 2015). The Wells-Riley equation calculates the probability for infection of a room inhabitant based on a number of parameters. Equation 1.1 demonstrates this probability calculation,

$$P = 1 - e^{-Iqpt/Q} \qquad (1.1)$$

Where P is the probability of infection, I is the number of infected people, q is the quantum generation rate, p is the breathing rate, t is the time of exposure, and Q is the outdoor air supply rate (ventilation rate) (Zhu, Srebric, Rudnick, Vincent, & Nardell, 2013) (Zhu, Srebric, Spengler, & Demokritou, 2012). This equation provides a calculable infection probability using parameters produced by this study. The combination of these methods can be applied to a space to determine the contamination likelihood of those in the room.

If the airfield in a room contains a contaminant, there are three ways in which the contaminant can be reduced or altogether removed to lower the probability of infection of the inhabitants, as determined by the Wells-Riley equation. These are source removal, disinfection, and dilution. The contamination under study are the bioaerosols emitted by people during respiration. Since the purpose of most indoor

spaces is to contain people, the source of the contaminant, source removal is not an option. Disinfection involves the deactivation of the contaminant. This can be done using ultraviolet light, which damages the microorganism's DNA, lowering its potential to cause harm. Lastly, dilution involves bringing in new air to the room to spread out the contaminants, reducing their concentration and effectiveness. This effect is achieved through efficient ventilation systems. Previous studies have examined the effect of fans in redistributing microparticles inside of a chamber, with the intent of pushing the potentially harmful particles to the upper portion of the room (Pichurov, et al., 2015) (Zhu, Srebric, Rudnick, Vincent, & Nardell, 2013). There, UV light would damage the bioaerosols and lower their potential to cause harm. Ideally, a space's ventilation system would propel the bioaerosols to a location where they can do less harm to the inhabitants. Whether that is to an outlet air vent or to the upper portion of the room where UV light deactivates the bioaerosols, this strategy must be kept in mind when designing for the airflow. These studies laid out a few key facts that influence the design of such a ventilation system:

1. Bioaerosols settle in the lower portion of the room (Zhu, Srebric, Spengler, & Demokritou, 2012).
2. The longer the microorganism is exposed to UV light, the higher the probability of its deactivation (Pichurov, et al., 2015) (Zhu, Srebric, Rudnick, Vincent, & Nardell, 2013).

Without a disinfecting agent, such as UV light or a ventilation filtration system, increasing the airflow rate was the most effective method of decreasing the probability of infection, as calculated with the Wells-Riley equation. If UV light was used,

however, this had the opposite effect, as the bioaerosols' exposure time to the radiation was critical (Pichurov, et al., 2015). In this case, it was more important to create an upward draft in the space, so that the microorganisms reached the area in which they were deactivated, but were not pushed out again before the light had time to damage their DNA.

This study has thus far reached the phase of flow rate calculations, a less precise method of developing ventilation rates than CFD, particle tracking, or the Wells-Riley equation, though that is perhaps most similar to the methodology used in this study. The work presented here is based primarily on two controlling equations, volumetric balance of airflow into and out of a space, and a contaminant balance equation dependent upon the same flow rates (Section 2.2). These both rely on perfect mixing within the spaces themselves, which is a simplification necessary for the scale of this work. Rather than determining the exact flow rates in and out of a single space, the team was more concerned with calculating approximate flow rates for 4- and 7-story dormitories with hundreds of rooms and occupants. Simplifying assumptions such as perfect mixing and the standardization of flow path leakage parameters, which were adjusted on a need basis during calibration of each individual zone. The initial parameters were based on the orifice type corresponding to each flow path, predefined in the CONTAM package.

1.5: Thesis Outline

1.5.1 Timeline of Events

Environmental monitoring sensors that track CO_2, temperature, relative humidity, and dew point were placed in 6 different buildings on the University of Maryland campus. These locations included classrooms, hallways, dorm rooms, and a rooftop. Two varieties were used, 65 wireless sensors and 89 Bluetooth sensors, in total, 154 sensors. The sensors took measurements every fifteen minutes recording data that was downloaded manually or via Bluetooth once a week. Occasional equipment malfunctions caused the sensors to go offline, but these lapses were discovered in the weekly downloads and efforts were made to get the sensors recording again as soon as possible, albeit with gaps in data. Despite timeline gaps, the sensors recorded instances of environmental data every 15 minutes from October 2017 to June 2018.

Drifts in the sensors' calibration occurred over time as well, lowering the accuracy of the data. Thus, the sensors were individually calibrated twice, once in January 2018 and again in June 2018, after the sensors had been taken down. The calibrated CO_2 data was recorded. Trends in the data were observed based on average values and the differences between both daily and nightly CO_2 concentrations, and occupied and unoccupied concentrations in each of the buildings.

Another aspect of the study involved calculating the actual ventilation rates in the two main dormitories, Building B and Building A, the low and high ventilation buildings, respectively. Information was taken from the buildings' mechanical drawings to create accurate multi-zone models of each. Calibrated using CO_2 concentrations from the non-occupied periods of time (e.g. spring break), the models

were then used to produce ventilation rates in each of the rooms that had a sensor during the spring semester. The trends based on these ventilation rates were evaluated and then compared to those apparent from the CO_2 study.

The third aim of the study was based on actual occurrences of upper respiratory illness during the spring semester. Volunteer participants in a study, called Characterizing and Tracking College Health (CATCH), by the Defense Advanced Research Projects Agency (DARPA), were asked to report any illness they felt they had at any time during the study period. qRT-PCR tests were performed off of swab, blood, and breath samples. This type of test was chosen for its sensitivity to influenza virus RNA (Ali T, 2004) (CDC, 2012). If the samples came back positive for any sort of respiratory illness, the most common being influenza, the participant was monitored until the virus left his or her system. Room numbers of the participants were tracked to observe the spread of cases to nearby rooms.

1.5.2 Overview

As part of this thesis, the team explored the association between indoor microbiomes and HVAC systems. In order to achieve the three study aims, a series of data sets were collected, including the CO_2 concentrations in the studied dormitories, ARI occurrences in the same dormitories, and window/door opening responses from occupants of those rooms that were infected. From these, the ventilation rates in the buildings were developed, and a correlation could be drawn between locations of low ventilation and ARI occurrence. The ventilation patterns were further used to predict the locations of potential ARIs due to cross-contamination between the rooms, and then compared to the actual results to evaluate the accuracy of the models. The window/door

responses were used to determine the changes in ventilation in a room due to the different schedules of opening windows and doors that the students reported. From these results, conclusions were drawn in support of the project hypothesis.

Chapter 2: Methodology

2.1: Environmental Sensors and CO_2 Collection

The first step taken in this multi-year project was to deploy sensors to gather environmental data in the two buildings of interest. 154 sensors in total were dispersed in rooms on the first through fourth floors of Building A, the high ventilation building, and on the second through seventh floors of Building B, the low ventilation building. The two types of sensors were the HOBO MX CO2 Logger (MX1102) Bluetooth sensor and the Paragon Robotics SC75 wifi sensor. The HOBO logger's CO2 sensor ranged from 0 to 5000 ppm, with an accuracy of +/- 50ppm. The Paragon Robotics logger's CO2 sensor ranged from 0 to10,000 ppm, with an accuracy of +/- 100ppm. The sensors were evenly distributed between the two buildings. Figure 3 shows the arrangement of sensors on the north end of the fifth floor of Building B, a typical distribution of both CO_2 and pressure sensors, which were used to calculate ventilation rates.

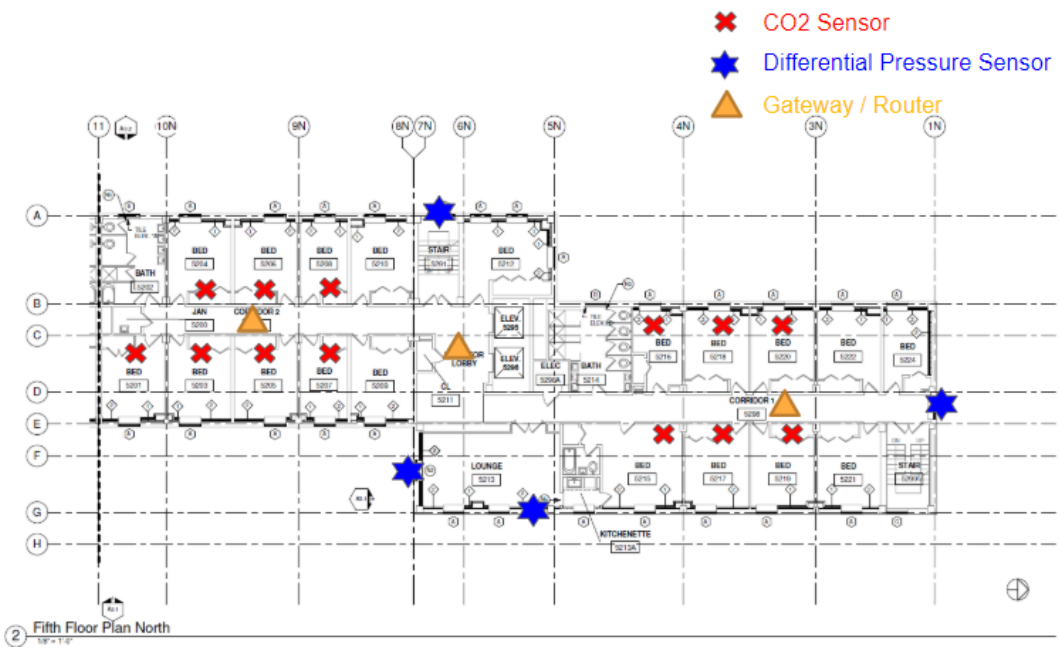

Figure 3: Sensor deployment plan for the fifth floor of Building B.

Environmental sensors were placed high on the wall, opposite the windows and next to the doors, to avoid being near student beds or desks and receiving direct contamination of exhaled CO_2. Increased sensitivity to airflow through open doors was a possibility, but would be less impactful to the measured values than direct airflow from a window or exhalation from the room's occupants. Pressure sensors, 6-8 per floor, were placed in common areas, lounges, hallways, or stairwells. It was assumed that students were less likely to open windows in these areas and skew the indoor pressure readings the sensors measured.

The environmental sensor array was composed of 65 wireless CO_2 sensors and 89 blue-tooth CO_2 sensors. A large number of sensors was chosen knowing that, over the months of data collection, some would become faulty and not be able to provide results for some or all of their life span, a hypothesis which proved accurate. However, reliable CO_2 data was recoverable from 38 of the sensors in Building A and 69 in

Building B, providing plenty of rooms for analysis during later steps in the study. Figure 4 shows one of the wall-mounted sensors, which display real-time data as well as storing it for future analysis.

Figure 4: HOBO data logging sensor (top) and Paragon Robotics logging sensor (bottom).

Between the initial data collection to set up and test the sensors and the primary data collection relevant to this study in spring 2018, the sensors gathered over 1.5 million data points. The sensors collected CO_2, temperature, pressure, and humidity data points every 15 minutes. Data collection began in October 2017 and ended in May 2018, but the data used in analyzing the buildings' ventilation and calibrating the

ventilation models was taken from the spring semester 2018 alone, from late January to early May 2018.

Though not used in this phase of a larger study, the temperature and relative humidity data can also provide indications of increased ARI exposure. Low temperatures have been found to cause increase in transmission. Humidity values between 20-35%, as well as above 80%, in turn decrease transmission (Lowen, 2007).

In order to use the CO_2 concentrations in analysis of the dormitories, each sensor was individually calibrated with a linear equation obtained from a correlation between known and measured CO_2 concentrations. Sensor calibration occurred at two points in time. Initial sensor calibration was done in January and final calibration in June 2018. The sensors were put in pressurized chambers for three hours at known CO_2 concentrations of 500, 1000, and 5000 parts per million (ppm). The average steady-state CO_2 concentration measured by the sensor was calculated for each known concentration and the points used to create a linear curve. The linear equations from each calibration period (January and May) were applied to the uncalibrated data as a time-step function, so that the initial and final calibration equations were not equally applied to each datum depending on the time span between calibration and collection of that datum. The following set of equations shows the two calibration curves and how they were combined to produce a time step equation that produced a calibrated CO_2 concentration (x) for each measured concentration (y).

Calibration curve 1: $y_1 = m_1 * x_1 + b_1$

Calibration curve 2: $y_2 = m_2 * x_2 + b_2$

Time step equation: $$x = \frac{N-n}{N} * \frac{y-b_1}{m_1} + \frac{n}{N} * \frac{y-b_2}{m_2}$$

Where n was the number of days from the sensor's initial calibration date, N was the total number of days between the two calibration dates for the sensor, m and b are the slopes and intercepts of the respective equations determined from the pressure chamber tests, and y and x are the uncalibrated and calibrated CO2 concentrations, respectively.

The analysis was taken further by using the CO_2 concentrations to find the actual ventilation rates in the rooms of the two dormitories. By finding the CO_2 concentration in each room when the residents were not present for an extended period of time, it was possible to find the CO_2 concentrations of an empty building, which could be represented by the multizone models. Baseline, or non-occupancy CO_2 concentrations were calculated by averaging the CO_2 values during school breaks, when concentrations were at their minimums and the air inside the rooms had a chance to reach near-equilibrium with the outside air due to the departure of residents for days at a time.

2.2: Ventilation Systems and Modeling

The main focus of this paper is the calculation and meaning of the ventilation rates in two dormitories. As previously indicated, CO_2 concentration in a space is used as an indicator of how much fresh air is entering a space and thus ventilation can be predicted. This is taken a step further with the actual calculation of ventilation rates and airflow between individual rooms, which can then be used to model and track the movement of contaminants such as ARI-causing viruses in the building. In order to calculate the ventilation rate, mass balance and airflow equations were incorporated

into the multi-zone model's algorithm to track the movement of air around the scaled buildings. In order to properly model the buildings, the existing ventilation systems were defined and broken down to be programed into the model. Once this process was completed, the buildings monitored were delineated by the predominant HVAC system installed. Table 1 provides the description of the types of ventilation systems in these buildings.

Table 1: Ventilation systems in the buildings studied.

HVAC Type	Descriptions
High Ventilation	• Utilize Dedicated Outdoor Air System (DOAS) with FCs or Central HVAC system.
Low Ventilation	• Use only Fan Coils Units (FCUs) and outdoor air from the open windows or infiltration.

Building A, with its newly installed DOAS, falls decisively under the category of a high ventilation building, especially relative to Building B, which relies on FCUs to heat/cool individual rooms. Each of the models was created in CONTAM, a computer program, designed by NIST, the National Institute of Standards and Technology, and used to analyze ventilation and contaminants of multizone indoor spaces. With access to mechanical schedules, floor plans, and building operation data, realistic multi-zone models were built for each room in both buildings. These models included all of the room volumes, openings (doors and windows), and mechanical ventilation equipment vital for the accurate calculation of ventilation rates. Other

estimates were also necessary for CONTAM to produce flow rates in and out of each room. These included leakage through the closed windows and doors, walls, and exterior surfaces. Though small, these numbers produced a more accurate model. Building A has at least one AHU on each of its four floors, and an air supply, in every student room, that produces 22-29 cfm of fresh air. The central system has an overall capacity of 10,000 cfm of air. Building B was built with four AHUs, three capable of pumping 3500-4500 cfm of air and one capable of pumping 12,200 cfm of air, in the basement and bottom floor. Approximately six exhaust fans populate each of the upper floors, but none in bedrooms.

The following two figures show representative floors in each models.

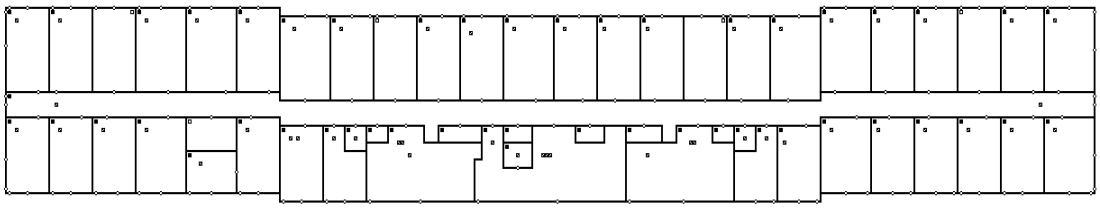

Figure 5: Building A floor plan for upper (resident) floors, as constructed in multi-zone model.

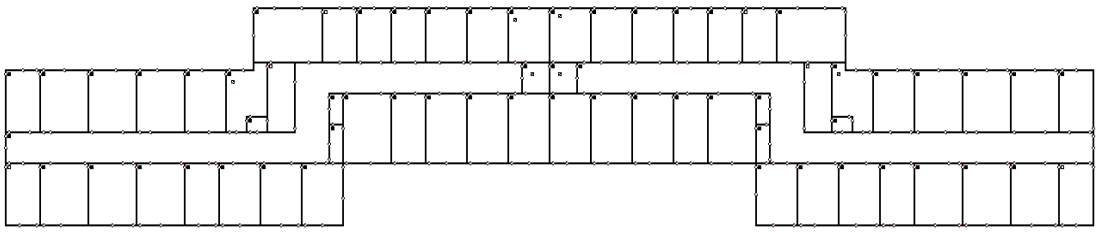

Figure 6: Building B floor plan for upper (resident) floors, as constructed in multi-zone model.

Despite the overall size difference between the two buildings, they have similarities in layout, building age and maintenance, and resident population density. The dormitories are adjacent to each other on the campus, so it can be assumed that their ambient CO_2 concentrations, temperatures, barometric pressures, and other weather phenomena are the same. This made them ideal for the comparative study.

The next step after calibrating the CO_2 data collected over the spring semester was to calculate the ventilation rates. The models of each dormitory shown above were created to aid the calculation of flow rates into and out of the network of rooms. The specifics of the different spaces were obtained from the building blueprints and mechanical drawings.

For each room with a sensor, the program was run over a given period of time to calculate the different flow rates in cubic feet per minute (cfm) through each opening or wall of the room, based on approximated leakage and orifice sizes. The ventilation rates were calculated by summing the flows in or out of the room for each room with a sensor and averaged over the given period of time, from January to May 2018. In order to convert units from cubic feet per minute to the air change rate per hour (ACH), the flow rates were divided by the room volume and multiplied by the conversion factor from minutes to hours.

The controlling equations for these calculations, shown below, are the volumetric flow rate equation, which equated the overall ventilation rate in and out of a room, and the source term equation, which uses the flow rates, contaminant concentrations (in this study, CO_2 and later influenza viruses), and a source flow term that accounts for sources of the contaminant within the space.

$$\dot{V}_{air,in} = \dot{V}_{air,out} \quad (2.1)$$

$$\dot{V}_{air} C_{CO2,in} + \dot{N} = \dot{V}_{air} C_{CO2,out} \quad (2.2)$$

Where $\dot{V}$ is the volumetric flow rate of air into and out of a room, C_{CO2} is the concentration of CO_2 (or any contaminant), and $\dot{N}$ is the source flow rate of this same contaminant. Equation 2.1 was the primary equation used in the calculation of ventilation rates based on flow paths, while equation 2.2 allowed for the validation of ventilation rates as well the calculation of the flow of airborne viruses between rooms.

2.3: Model Setup

The first step in the calculation of ventilation rates was to set up the multizone models for the opposing buildings. This procedure involved the incorporation of the buildings' mechanical specifications into CONTAM, the program designed to calculate flow rates from a given model. The buildings were first drawn as a two-dimensional floorplan, floor by floor, to produce figures like those shown in Figures 5 and 6. Each room, or zone, was drawn arbitrarily, without concern for exact scale given the larger overall scale of the buildings themselves. The room areas and heights were then individually programmed into the model so that the volume of each bedroom, bathroom, lounge, hallway, or other space could be determined. After the physical borders of the dormitories' interiors were drawn, the flow paths were added in to allow the full calculation of the ventilation rates.

Two different models were originally created, one with closed flow paths (closed windows/doors) and another with open flow paths (open windows/doors). The

flow paths, also individually defined and placed, included not only windows and doorways, but also leakages in the interior and exterior walls. The type of orifice was largely irrelevant, as the calculation of the airflow through each was determined by the leakage area of the item (doors and windows), in cm^2, or the leakage area per unit area (interior and exterior walls) in cm^2/m^2. Wall leakages, however, did not change between the open and closed flow path models. Between the two primary dormitory models there were over 20 different types of flow paths defined, initially. In the model calibration another 8 were produced to account for larger and smaller leakages in doors, windows, interior walls, and exterior walls that could more accurately produce the expected non-occupancy CO_2 concentrations. Figure 7, which shows a room from the closed flow path model, presents a room with 6 different flow paths. In all, Building A had 229 zones and 983 flow paths. Building B had 529 zones and 1836 flow paths.

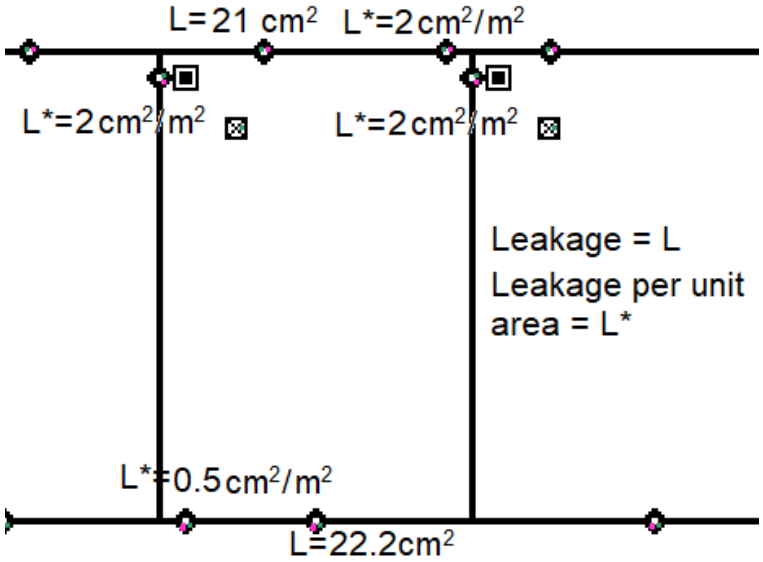

Figure 7: Closed flow path room in Building A.

To model open flow paths, the paths could be redefined for larger leakages. For example, the same room from Figure 7 is again shown, below in Figure 8, with open flow paths.

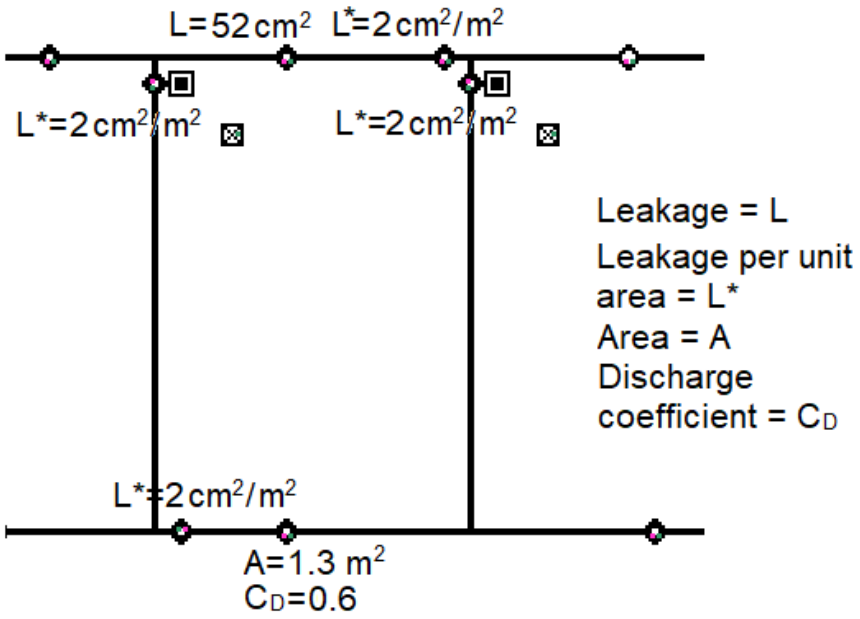

Figure 8: Open flow path room in Building A

In this model, it was assumed that the doors were open at 45 degrees and the windows halfway, standardized for simplicity based on observation of the two dormitories. The primary difference is in the definition of the window flow path. Rather than a leakage area, the item area is described based on the size of the open portion of the window for that room, along with a discharge coefficient, which relates the actual flow rate through the actual orifice size to the theoretical one (Haghighat, 2004). This allows for a prediction of one-way flow using flow power law. Equation 2.3 shows the role of the discharge coefficient in the determination of the flow rate through the opening.

$$\dot{V} = C_D(\Delta P)^n \qquad (2.3)$$

Where $\dot{V}$ is the volumetric flow rate, C_D is the discharge coefficient, ΔP is the change in pressure between the inside and outside spaces, and n is the flow exponent.

C_D is set to 0.6, n was set to 0.5, and ΔP depended on the internal-external pressure gradient for the particular window.

The third component of the building models were the ventilation systems themselves. In this aspect, the two dormitories differed the most. Building A had an AHU on each floor, while Building B had four AHUs on the bottom two floors only. Both buildings had exhaust outlets in larger rooms such as the community bathrooms and some of the lounges and study rooms. These were defined as air outlets, one-way flow paths that took in a prescribed volume of air per minute. The main difference was that Building A's individual bedrooms each contained a fresh air supply as well, set up opposite to the exhaust outlets. They were defined as one way flow paths into the rooms, the amount of airflow corresponding to that defined in the mechanical drawings, in cfm.

The contaminants had to be defined to allow CONTAM to correctly interpret units of input contaminant concentration or contaminant source rates. The two contaminants modeled in CONTAM were carbon dioxide, for the models' calibration and again in the production of ventilation rates, and influenza A, in the cross-contamination model. Influenza A was chosen to represent the viral pathogens detected by the qRT-PCR tests, as it was one of the more common viruses detected. CO_2 concentration was input as a concentration measured in ppm. To calibrate the models, the source term of Equation 2.2 was assumed to be zero and the input CO_2 concentration was the ambient concentration, 450 ppm. This concentration value was selected by averaging the concentrations detected over the semester by the outdoor sensor placed on the roof of the building between Buildings A and B. The sensor collected data from

November 2017 to June 2018. This outdoor CO_2 concentration also agreed with previous literature approximating the outdoor CO_2 concentration in semi-urban areas (George, 2007). In the calculation of the actual ventilation rates, produced for the spring semester and represented in Figures 15 and 16, the CO_2 concentration inputs were the collected and calibrated CO_2 values summarized in Figures 11 and 12. In cross-contamination modeling, the influenza virus was expired from residents within the room itself. This made it a source flow, measured in cfu/hr. This converted into cfu when multiplied by the output air mass flow rate, measured in ACH for consistency.

The complexity of the models is reduced greatly when focusing on a smaller set of rooms. In modeling the movement of the flu virus in three of the rooms where ARI's were detected within a week of each other, the only flow paths considered were those connecting the source rooms and those nearest to them on that floor. As distance from the source room, where the ARI was initially detected, increases, concentration of virus decreases rapidly, so that at most, only that floor needed to be analyzed.

Lastly, the weather and collected CO_2 data were converted to compatible files and input into the CONTAM program. Weather data, which included ambient pressure, affected the flowrates through exterior orifices, especially in the case of open windows. CO_2 data were converted to a set of contaminant files, which provided the ambient CO_2 concentrations for the transient ventilation rate calculations. The program was run for each room that had contained a sensor, since the actual CO_2 concentrations, and therefore actual ventilation rates, could not be predicted for those without.

To produce the primary result of the ventilation portion of the study, average seasonal ventilation rates observed in Figures 15 and 16, a simulation was run using

input data from January to May, to model the passage of the entire semester. A weather file was incorporated to model accurate transient pressure and temperature data. The simulation was run for each building, and the air flow through each flow path in each room was summed and averaged for the four month time period. An average ventilation rate, the sum of the flows into the room, was produced for each room.

2.4: Model Calibration

In order to ensure that the flow paths in the two multi-zone models numerically represented the actual air flow rates in the two dormitories, the non-occupancy CO_2 concentrations were calculated, using the models, for each room and compared to the measured non-occupancy CO_2 values extracted from the sensor data. The measured concentrations were calculated by taking the mean of the lowest third of data measured by a sensor during a time when the residents were known to be gone for that entire period, i.e. spring or winter break, depending on data availability. Even after the residents departed, it took a variable amount of time for the CO_2 concentrations to reach near-ambient concentrations, so the data selected was taken 2-3 days after the decrease in CO_2 values began, and only the bottom third of the data were averaged to reduce fluctuations in sensor readings.

The comparative model-calculated CO_2 concentrations were then calculated with the use of equations 2.1 and 2.2. The flow rates through each of the flow paths were summed using an input CO_2 concentration of 450 ppm, the steady state ambient CO_2 concentration, and a source term of zero, since non-occupancy was assumed. The output of the equations, $C_{CO2,\,out}$ was compared to the sensor measured CO_2 data value for the given room, and if the numbers varied by greater than 50%, the orifice sizes and

leakages were altered in the model until the difference between the calculated and measured values was smaller and thus, more precise.

Figures 9 and 10 show the differences in measured and calculated CO_2 concentrations as determined with the use of the models, after calibration. The rooms selected are a sample of twelve randomly selected rooms from each building.

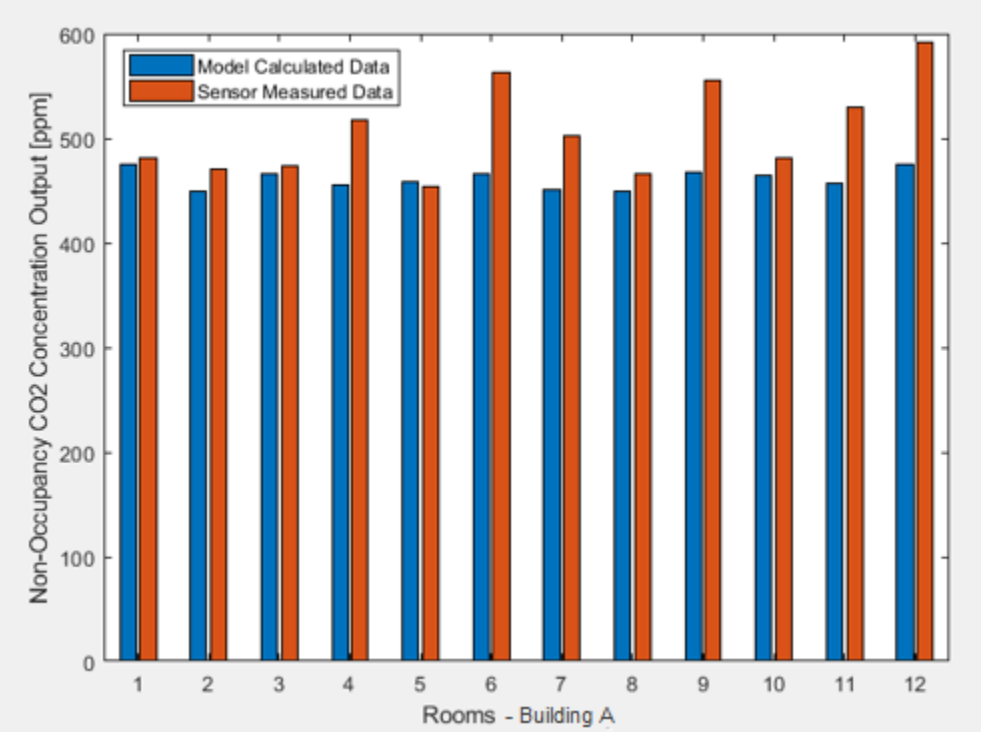

Figure 9: CO_2 sensor-measured and ventilation model-calculated concentrations of CO_2 during a non-occupancy time period in Building A.

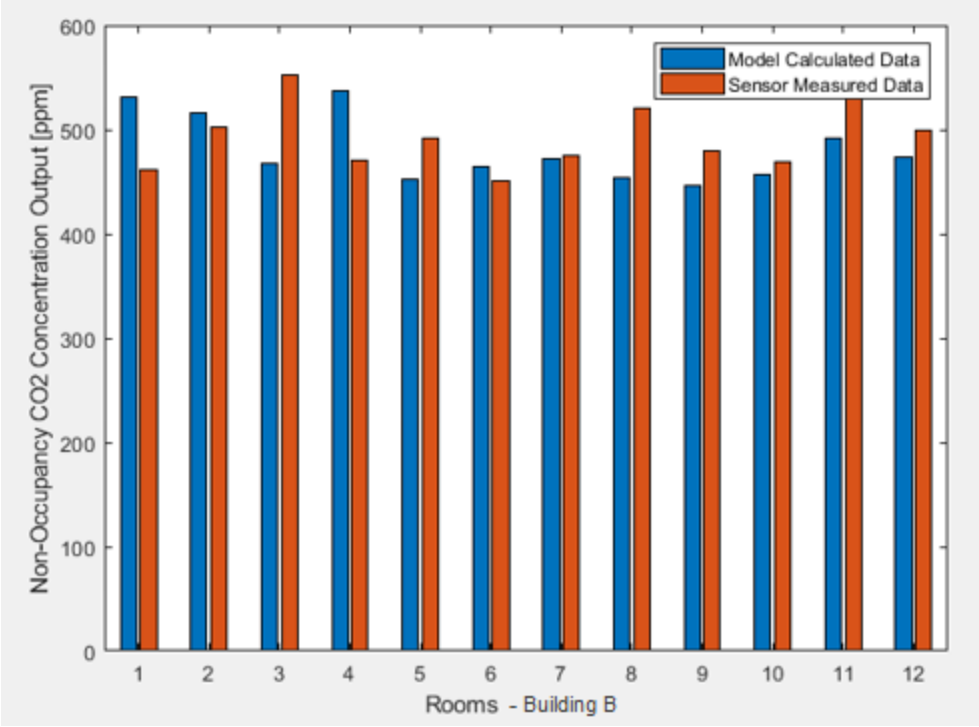

Figure 10: CO_2 sensor-measured and ventilation model-calculated concentrations of CO_2 during a non-occupancy time period in Building B.

The average percent difference between the sensor-measured and model-calculated data was 18.1% for Building A and 11.6% for Building B, post calibration. Given the expected imprecision of a model of this scale, this level of accuracy was sufficient to produce valid ventilation rates for the dormitories.

After model calibration verified the accuracy of the flow paths, the ventilation rates were calculated for the spring semester. This was done for each room. CO2 concentrations were input as transient contaminant data and the flow rates were calculated for each flow path, and summed to result in $\dot{V}_{out}$, the output flow rate that was then averaged to produce the results shown in the following section.

2.5: Window/Door Surveys and ARI Detection and Verification

Aside from the output of the environmental sensors and CONTAM models, two additional data sets were used in the analysis of ventilation and ARI occurrence. The first was a survey distributed to participants of the study in both dormitories. This survey asked a series of questions regarding the frequency and length of time that students opened their windows and door. The set of questions were as follows:

1. Did you have the window in your dorm room open during the night?
2. During the last 24 hours, while you were in your dorm room, did you open the window? About how long did you have it open?
3. During the last 24 hours, while you were in your dorm room, did you open the door and leave it open? About how long did you have it open?

The window/door opening survey was sent to all of the participants of the CATCH study, the same set of students who were monitored for ARIs by the School of Public Health. It was meant to be filled out separately by the students for each day they participated. 25 responded, 23 of which were in Building B and 2 were in Building A. Both of the rooms in Building A that filled out the survey were the two rooms were ARIs occurred. Of the 23 rooms in Building B who responded, 14 were in rooms where ARIs occurred. This majority showed a selection bias by the participants, who were more likely to answer the questions about their current window/door habits if ill.

These data were used to determine a schedule for window/door openings in CONTAM to model more accurate ventilation rates and compare ARI case rooms to rooms without illness. For representation of the results in CONTAM to be accomplished, assumptions were made. Having an open window was assumed to mean

that the window was halfway ajar, reducing the orifice size to half of the size of the window frame. An open door was assumed to mean that the door was held open at 45 degrees.

The other set of data collected was the reporting and verification of ARIs in the two dormitories. The cases were initially self-reported, but lab-verified. Residents of Buildings A and B were notified of the study through classes, emails, social media, and community events at the beginning of the semester. After filling out a brief survey, participants were encouraged to contact the study team via phone or email to let them know if they were ill. A compensation of $10 was used as additional motivation for participants. They were then asked about the timing of their symptoms, and had they begun within the past 36 hours, the students would be scheduled for a visit to the research team's clinic later that day. There they would provide nose and throat swabs, blood, and an expired breath test. A multiplex qRT-PCR tested their samples for evidence of infection with any of a number of viral pathogens commonly implicated in acute respiratory illness.

The high level of validity to these tests was offset by the initial self-reporting that brought students into the clinic. One problem was that of students who waited too long to report. If samples were collected outside of the 36 hour window, the chance of the qRT-PCR test detecting the virus was greatly diminished. There was also a selection bias of those who decide to report their illness. Most significantly, in theory, was the nature of the residents of the two dormitories themselves. They contain living learning communities, Business in Building A and Life Sciences in Building B. The health team believed that there was more interest among members of the Life Sciences community,

and therefore Building B, about the study, which had the potential to skew the number of reported ARIs in Building B's favor.

Chapter 3: Results

3.1 Carbon Dioxide Concentrations

CO_2 collection provided data consistently from the deployment of the sensors until their removal from Building A and Building B in May 2018. The data was collected every week but the results were not compiled until the end of the collection period. At this point, the second data calibration was performed on the sensors and then the two linear curves, one from January and the other from June, were applied to the raw data to improve its accuracy. The results of the sensor calibration are observed in Figures 11 and 12.

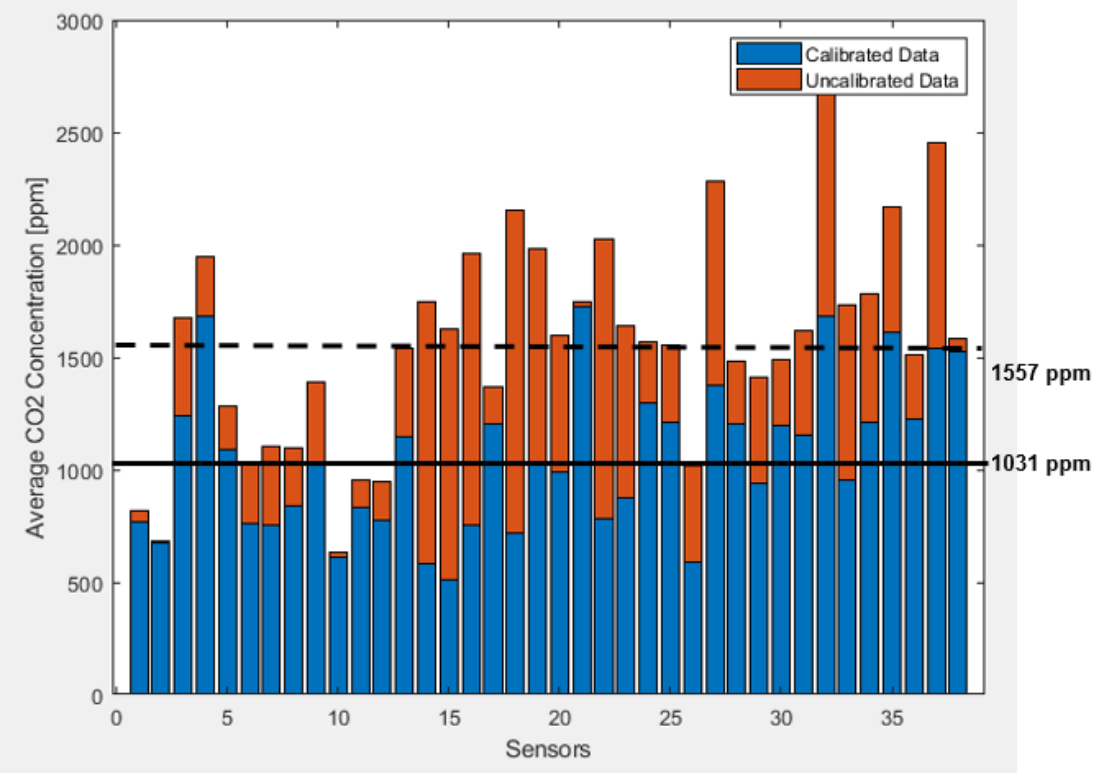

Figure 11: Average daily CO_2 concentrations measured by sensors in Building A. The solid line denotes the overall calibrated average of 1031 ppm. The dashed line denotes the overall uncalibrated average of 1557 ppm.

The concentration data vary dramatically, even after careful calibration of the individual sensors upon the completion of data collection. These data were collected in one semester, starting just before the return of student on January 24th to the semester's end, May 5th. Gaps existed in the data where sensors had gone offline or filled their data capacity and overwrote a subset of previous data. In addition, student habits produce large differences in the overall averages of the data. The amount of time the students spent in the room, their habits of opening and closing windows and doors, the number of visitors they had, and individual's breathing rates, control the quantity of CO_2 in individual rooms and cause the range to stretch from 546 ppm to 2269 ppm. Because months of CO_2 concentration data from 38 sensors in Building A and 69 sensors in Building B had been collected, the overall average concentrations after sensor calibration were an accurate indication of the ventilation in each building. The overall CO_2 concentration average in Building A was 1031 ppm (Figure 11). Building B had a significantly higher CO_2 concentration average of 1512 ppm (Figure 12).

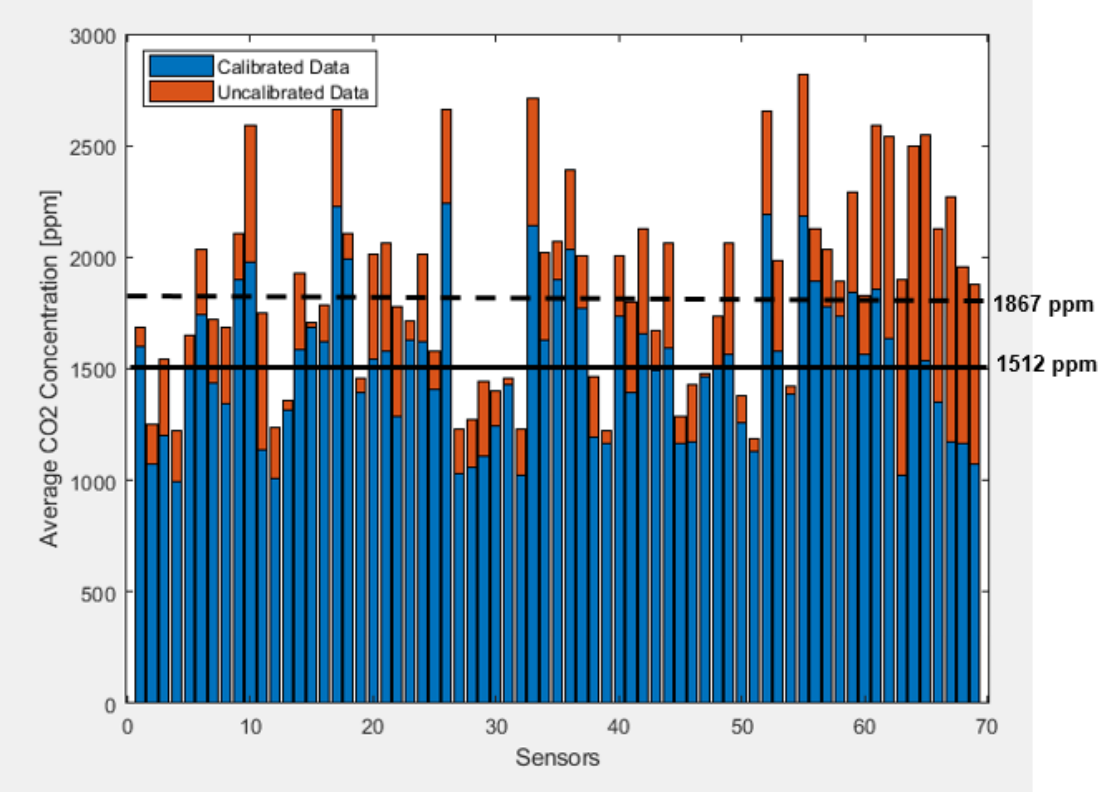

Figure 12: Average daily CO2 concentrations measured by sensors in Building B. The solid line denotes the overall calibrated average of 1512 ppm. The dashed line denotes the overall uncalibrated average of 1867 ppm.

The degree to which a sensor had to be calibrated depended on the individual sensors, but in many cases, as seen above, it reduced the CO_2 concentration values by more than 100%, apparent in Building A sensors 14 and 15. Other needed very little calibration, for example Building A sensors 1 and 2. Time caused degeneration in the sensors, making their calibration crucial in order to have reliable data.

Fluctuations within a single room's CO_2 concentrations were just as important to evaluate as the differences between the rooms. Regardless of the ventilation system, CO_2 concentrations increase during times of increased occupancy, especially at night, when the residents of the room were, typically, all present for an extended period of time compared to daytime. In order to evaluate the difference between day and night

CO2 concentrations, the data collected by the sensors between 0000 and 0600 hours, the "nightly" averages, were calculated. These were compared to the "daily" averages, which were the same as the overall averages, collected at all times of the day. These resulted in a total nightly average of 1092 ppm for Building A and 1740 ppm for Building B, higher comparatively than the daily averages of 1031 ppm for Building A and 1512 ppm for Building B. Appendix B shows the nightly and daily concentrations for each sensor in the two buildings.

Another analysis of fluctuation was done by determining the deviation in the data, shown graphically with boxplots. Each plot demonstrates the breadth of CO_2 readings gathered by each sensor. The following data are taken from a sample of twelve rooms in each building, evenly spread across the available floors, for a week of time. Figure 13 displays the standard deviations in CO_2 concentration for these twelve randomly chosen sensors from the Building A sensor array. Figure 14, similarly, shows deviation in twelve sensors from the Building B array.

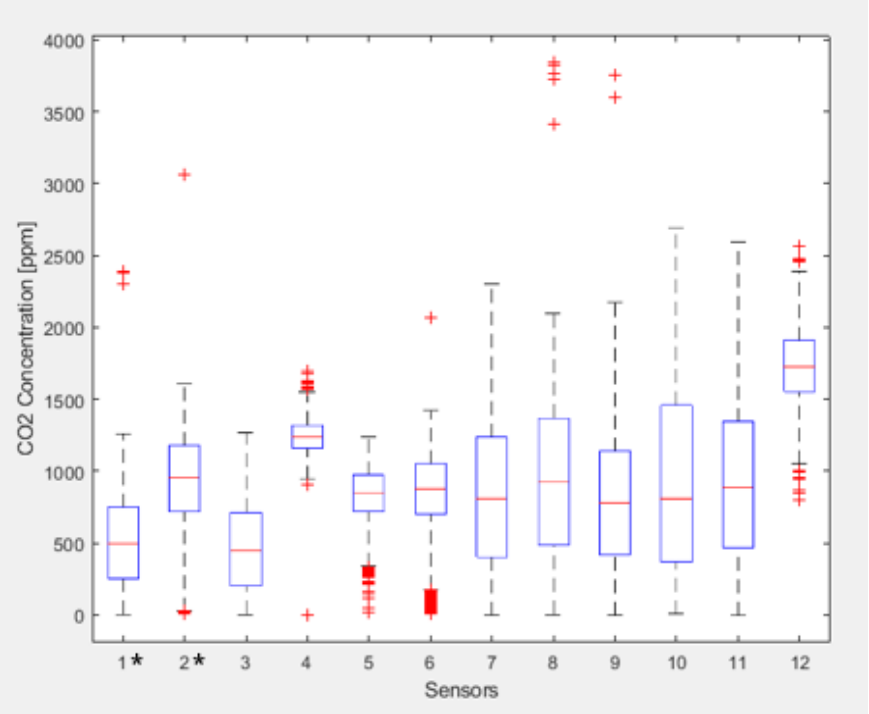

Figure 13: Box plots showing spread of CO_2 concentration data from 12 calibrated sensors in Building A. Asterisks denote sensors in rooms with ARI occurrences.

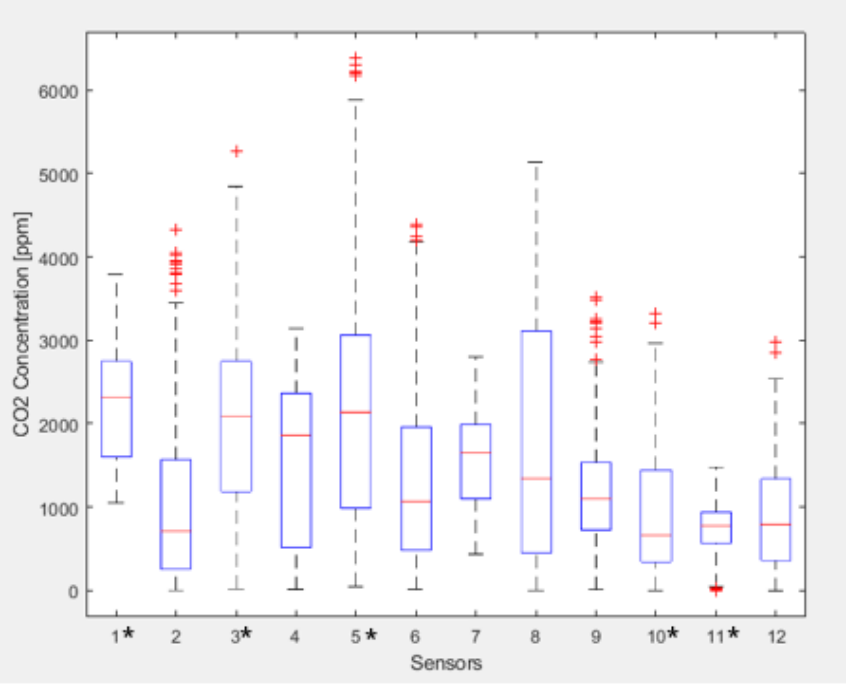

Figure 14: Box plots showing spread of CO_2 concentration data from 12 calibrated sensors in Building B. Asterisks denote sensors in rooms with ARI occurrences.

Even within a single week, the data measured by each sensor tended to vary greatly. The average standard deviation of CO_2 concentration data from Building A's sensors was 453 ppm. Building B's CO_2 concentration values had a standard deviation of 796 ppm. Appendix C shows the data for all of the sensors in both Building A and Building B dormitories, for the entire spring semester collection period.

3.2: Ventilation Rates

The CONTAM models were used to produce ventilation rates for the two dormitories. By summing the flow rates estimated for each room's flow paths, in and out volumetric flow rates could be determined, measured in cubic feet per minute. These volumetric flow rates were non-dimensionalized as the air change rate per hour by dividing the flow rate by the room volume and multiplying by 60 minutes per hour. This value was utilized in the cross-contamination analysis.

Hourly flow rates were produced for each flow path, which were then summed and averaged to determine the ventilation rate per room for the spring semester. The initial results were calibrated using the non-occupancy CO_2 data to validate the flow rates for each orifice and produce accurate overall ventilation rates for each room. The results of these calculations are shown in Figure 15 (Building A) and 16 (Building B).

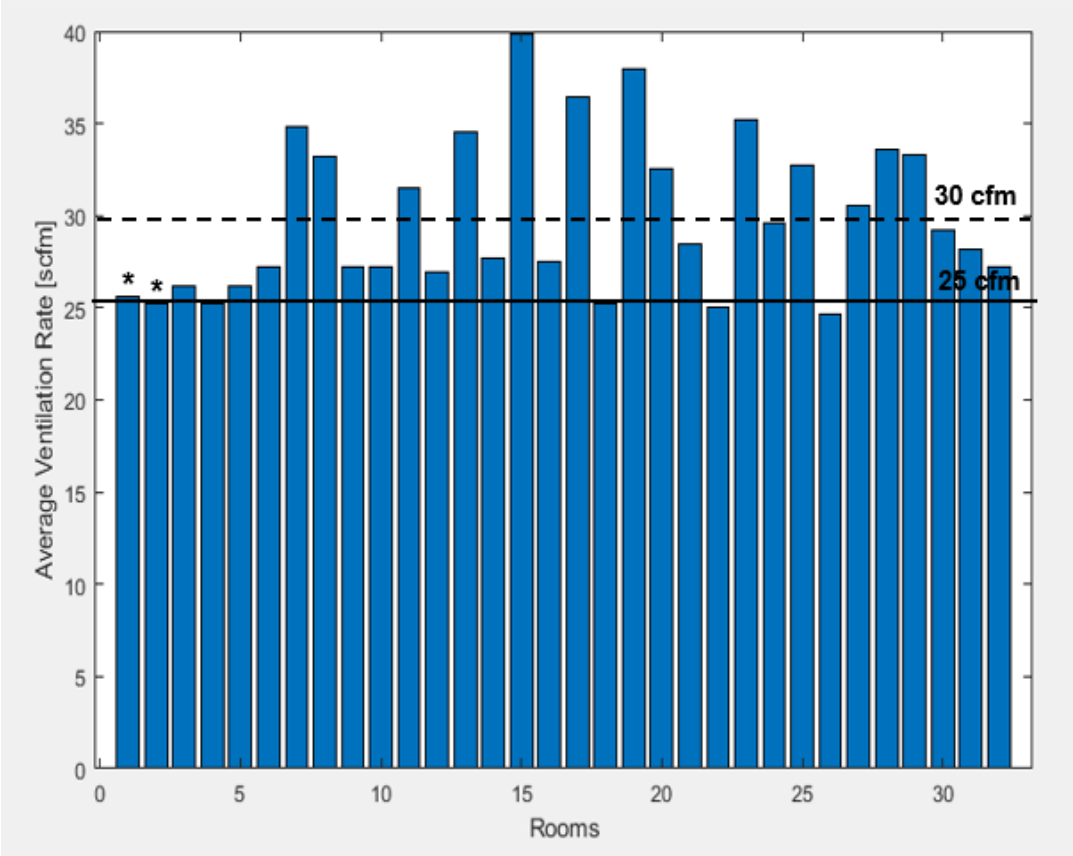

Figure 15: Average seasonal ventilation rates in rooms with sensors in Building A. The overall average ventilation rate was 30 cfm (dashed line), while the ventilation rate average in the sick rooms, denoted by asterisks, was 25 cfm (solid line).

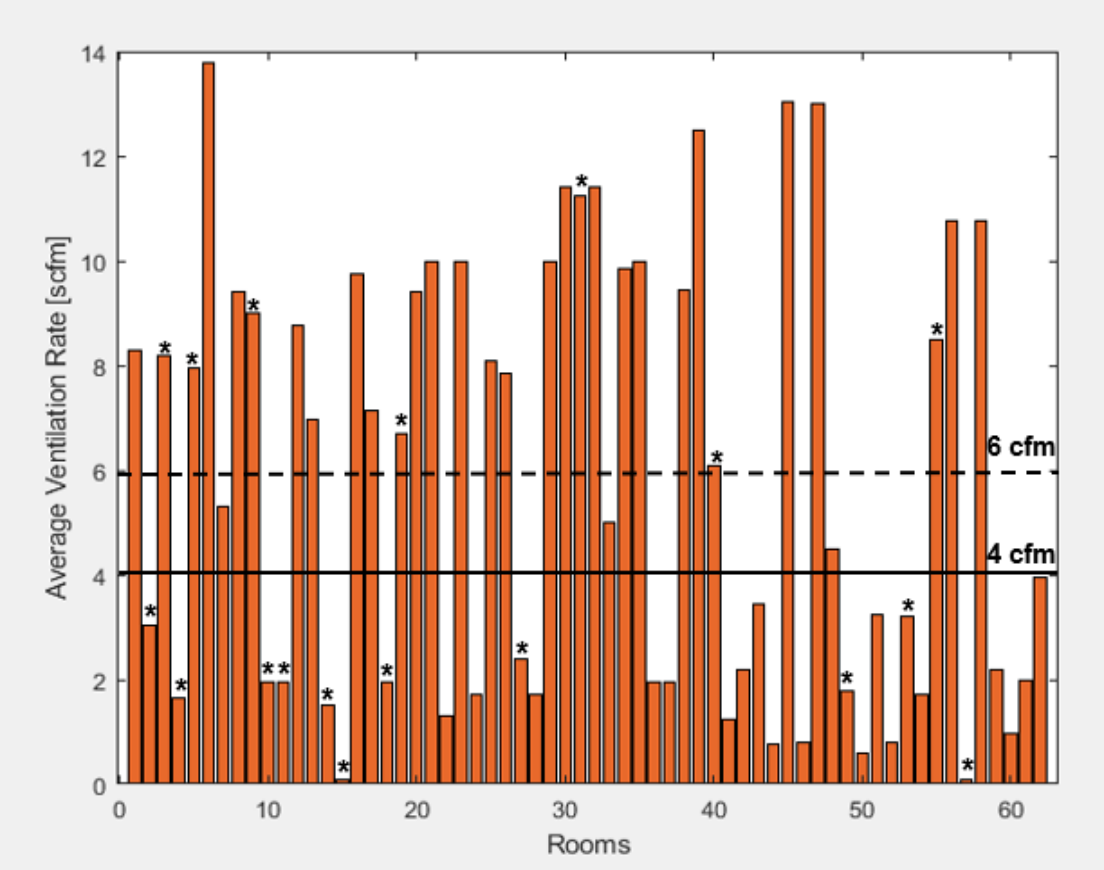

Figure 16: Average seasonal ventilation rates in rooms with sensors in Building B. The overall average ventilation rate was 6 cfm (dashed line), while the ventilation rate average in the sick rooms, denoted by asterisks, was 4 cfm (solid line).

These data provide a number of immediate observations about the two buildings. Building A had higher ventilation rates, both as an overall average of 30 cfm compared to Building B's 6 cfm, and individually, room-to-room. The highest calculated ventilation rate in Building B was 14 cfm, while the lowest in Building A was 24 cfm. In both buildings, the average ventilation rate in rooms with ARI occurrences was lower than the overall average. Building A's average ventilation rate for its two rooms with ARI's was 25 cfm while Building B's average ventilation rate for its twenty rooms with ARI's was 4 cfm.

While Building B's rates vary greatly from room to room, Building A's are all above 22 cfm, which was the minimum quantity of fresh air pumped into any room by

the building's centralized ventilation system. Further variation above 22 cfm is a result of infiltration. Infiltration, however, provided all of the ventilation in Building B, where there was no air brought in by the building's mechanical systems. Because of this, there is no minimum threshold, as can be observed by looking at rooms 15 and 57 (Figure 15), where ventilation is nearly nonexistent. It can be hypothesized that these rooms rarely, if ever, kept their windows and doors open.

3.3: Analysis of Environmental Data and ARI Cases

The third analysis conducted compared the overall average ventilation rates in the two contrasting dormitories to the number of ARIs reported in each. The average ventilation rates, reported in Figures 15 and 16, demonstrate the success of DOAS in introducing fresh air to Building A relative to infiltration ventilation, the only source of fresh air in Building B, but the importance of fresh air is emphasized by the ARI results. Table 2 summarizes the number and location of ARI cases by dormitory between January and May 2018.

Table 2: Respiratory illness statistics comparing the two dormitories, with high and low ventilation respectively.

Student Dormitory	Number of Recorded ARI Cases	Total Dormitory Population	% of Dormitory	Average Ventilation Rate (Spring '18)
Building A (HVB)	2	223	1	30 cfm
Building B (LVB)	30	545	6	6 cfm

Building B had 15 times as many ARIs during the 2018 spring semester as Building A. Factoring in Building B's larger resident population, the poorly ventilated dormitory still had 6 times the number of ARI occurrences. This corresponded to an average student room ventilation rate that was 5 times lower than the ventilation rates in Building A.

3.4: Cross-Contamination Cases

While ventilation cannot prevent dormitory residents from acquiring infections in other locations, such as classrooms, the library, and friends' rooms in other buildings, indications that the ARI came from within the dormitory itself are the timing of ARI diagnosis and physical location of rooms with other ARI cases. Five sets of cross-contamination cases, defined as dormitory residents who acquired ARI from another resident in close proximity based on timing of lab-positive ARI report, were identified by assessing the date and physical location of ARI detections. In these scenarios, it is likely that the source case acquired ARI outside the dormitory, and due to low air turnover, the virus spread from room to room during a limited time period of approximately one week.

All cross-contamination cases were identified among Building B residents, as the only two incidences of ARI in Building A occurred a month and a half apart. Among Building B ARI cases, two clusters of cross-contamination cases occurred in February, two in March, and one final cluster in April. Each cluster involved three or more rooms on the same floor, generally within 4 rooms from the source (defined as the lateral distance from the source room, or from its opposite across the hall). This distance was experimentally determined to be the maximum distance in any direction (dependent on

net flow rate directions) from the source room that a detectable (>.125 cfu) virus concentration was calculable *by the models*. This distance estimated the actual contamination radius of the source rooms, using a constant virus source term. The specific strain of virus was also documented, to track the change in the virus as it travelled between cases. In addition, 4 of the 5 clusters involved cases where the same or a different occupant of the source room had a positive lab result again within a week of the first ARI detection in that room, indicating that there was still a significant concentration of virus in that room.

The clusters were further analyzed to model the spread of ARI-inducing virus from the source room into the surrounding rooms. The first cluster model used the results of a survey distributed to all of the rooms when and where an ARI occurred, as well as a few other rooms selected at random. This survey asked the occupants whether or not they kept their door open during the day and their windows open during the day or during the night. If they answered yes, the occupants were asked to given an estimate of the length of time the door/windows remained open. The questions were repeated for each day that the room contained a sick occupant, someone who had positive lab results. These answers would have impact on the flow paths and thus the ventilation rate of the room. Based on these resident self-report surveys, the members of the first cluster, shown in Figures 17 and 18, kept their doors open during the days in which ARIs were detected, a habit unique to that cluster alone, and potentially a cause of increased virus concentration in the neighboring rooms, as the flow rates between them could increase. It was modeled twice, once with closed windows/doors, and again with open doors corresponding to the number of hours/day that the occupants had indicated

that they had kept their doors open (Section 3.5, Table 2), according to the survey results. All three rooms where an ARI occurred kept their windows closed during the week of infection, limiting their supply of fresh air. In addition, the room occupants kept their doors open a reported 2-5 hours a day, which would increase ventilation but not to fresh, outside air, air that carried the flu virus. Figure 17 shows the rooms and corresponding virus concentrations in Cluster A when the doors were closed, while Figure 17 shows a similar, open door simulation. (SGL=single room, DBL=double, TRP=triple, QD=quadruple, BTH=bathroom, *=ARI occurrence)

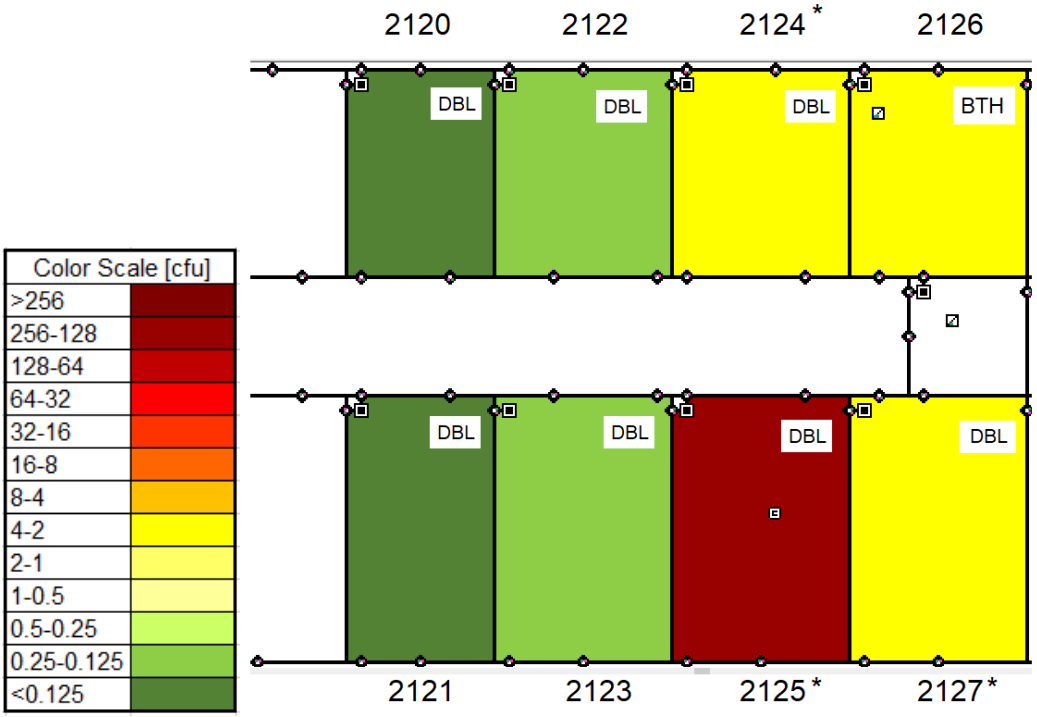

Figure 17: Simulation of the spread of influenza A in rooms surrounding source room, 2125. The colors, defined in the logarithmic scale to the left, show the concentration of virus in cfu after two days. In this simulation, the doors are closed.

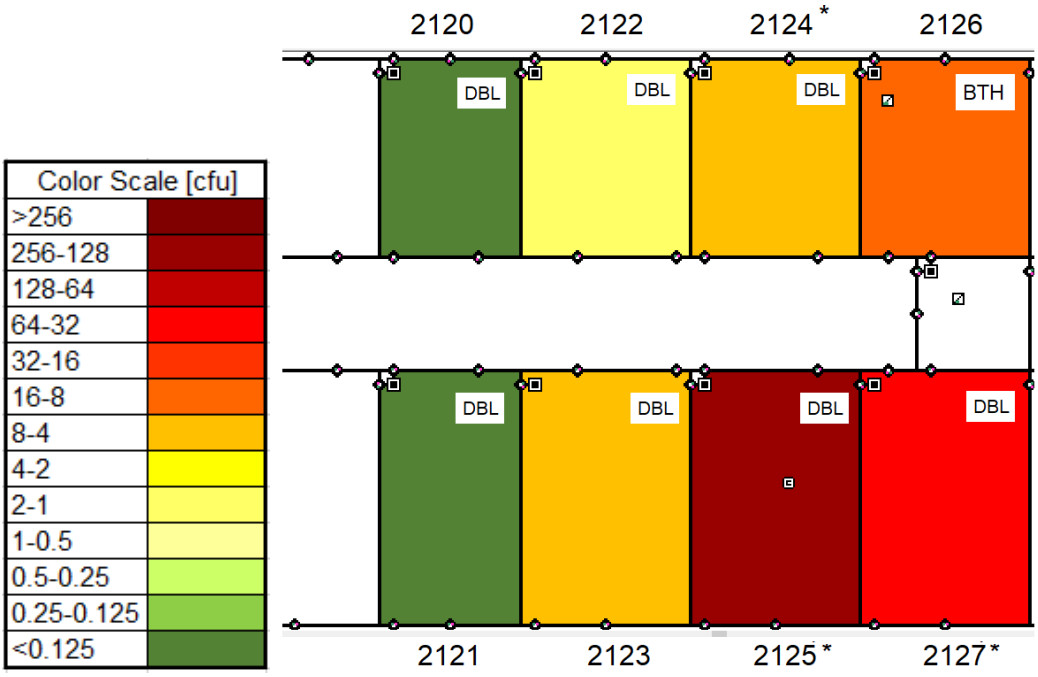

Figure 18: Simulation of the spread of influenza A in rooms surrounding source room, 2125. The colors, defined in the logarithmic scale to the left, show the concentration of virus in cfu after two days. In this simulation, doors are open.

The estimated source (virus) flow rate was 60 colony-forming units per hour (cfu/hr), and this number was the source term, $\dot{N}$ from equation 2.2, used in the simulation. The ventilation rates over the week of infection, February 7th to February 15th, were calculated and used to map the flow of air and contaminant between rooms. Steady state concentration was reached after 9-12 hours.

The first, closed door simulation, resulted in the virus concentrations shown graphically in Figure 17. The source room had a steady state virus concentration of 219 cfu after the 48 hour simulation period. Rooms adjacent to the source room, 2127 and 2123, had 3.0 and 0.2 cfu respectively, while rooms across the hall, 2122, 2124, and the bathroom, 2126, had 0.2, 3.9, and 2.9 cfu, respectively. Rooms outside of this radius had less than 0.125 cfu.

The second, open door simulation resulted in higher flow rates through the flow paths corresponding to doors, and therefore higher concentrations of virus in rooms with a net inward flow rate through the door. Rooms 2123 and 2127 had 8.2 and 57.4 cfu respectively, while rooms 2122, 2124, and 2126 had 1.8, 9.0, and 8.9 cfu respectively. The source room had a lower viral concentration of 188 cfu, due to the increase in airflow because of open doors, even though the effect was simply to pass on the airborne disease to neighboring rooms. Despite the increase in concentration in adjacent rooms in the second simulation, the pattern of contamination does not correlate with ARI case rooms as well as the first simulation. This indicates that transmission occurred at night, when doors were closed and residents were all present, sleeping and breathing at a constant rate, similar to the constant simulation source flow.

The other four clusters were also modeled with closed window/door flow paths. The results are shown in the following four figures, 19-22, with varying success as to the prediction of ARI occurrence based on flow path modeling alone.

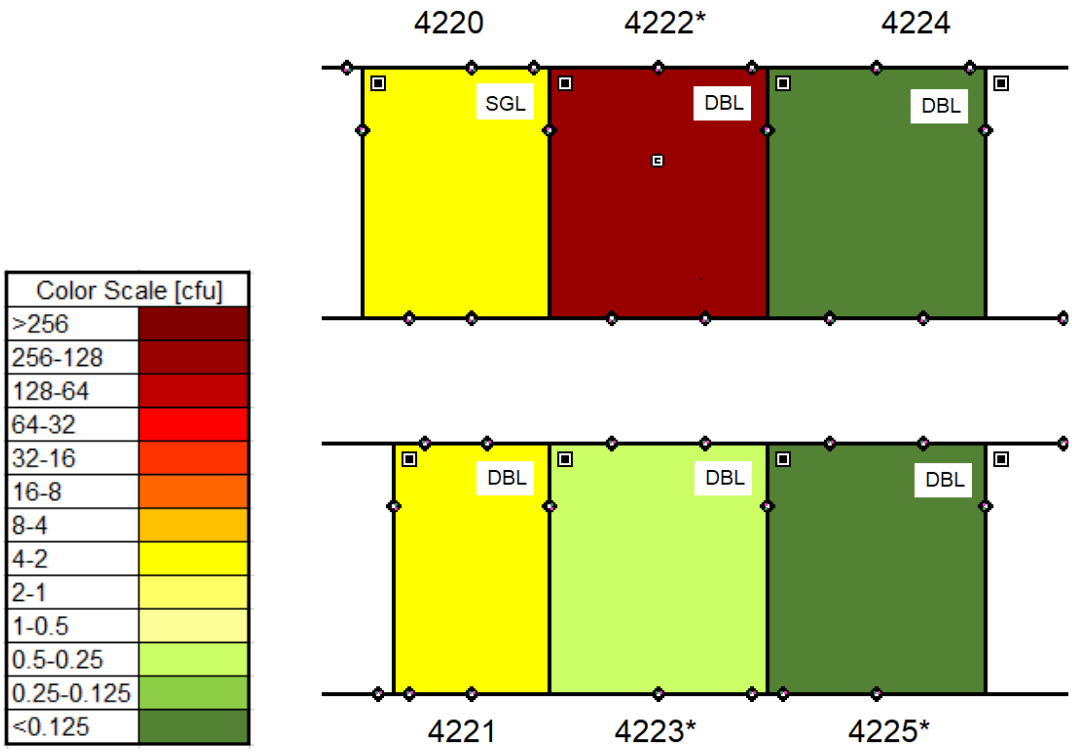

Figure 19: Simulation of spread of virus in rooms surrounding source room, 4222. The colors, defined in the logarithmic scale to the left, show the concentration of virus in cfu after two days.

As with cluster A, the source term used in the modeling simulation for clusters B-E was 60 cfu/hr. The model simulated two days, and steady state virus concentrations were reached after a maximum of 12 hours. The modeled flow of virus in the B cluster demonstrates a left- and downward ventilation pattern, relative to the viewer. Room 4222 had outward flow paths into room 4220 and the hallway, where rooms 4221 and 4223 were recipients of the airflow, due to their inward flow paths. Room 4223 received a steady state virus concentration of 0.3 cfu. The air exchange with room 4223 accounts for the ARI incident in room 4223, but the occurrence in 4225 is more difficult to account for. It is possible that the occupants of 4225 spent time in one of the other two incident rooms or in the company of the one or more infected occupants. Or, alternatively, that the directional flow rates are not correctly predicted by the model, as

the rooms where actual ARI detection occurred are in the opposite direction as the simulated flow. Rooms 4220 and 4221 received 2.8 and 2.1 cfu of steady-state virus concentration, respectively, after 9 hours (i.e. the time it took for the model to reach steady state). According to the simulations they should have had an increased likelihood of contracting the virus, but no ARI was detected in either. Regardless of the reason, the model does not as accurately predict the behavior of viral flow for Cluster B as it did for Cluster A.

Cluster C, another set of three ARI cases, is shown in Figure 20.

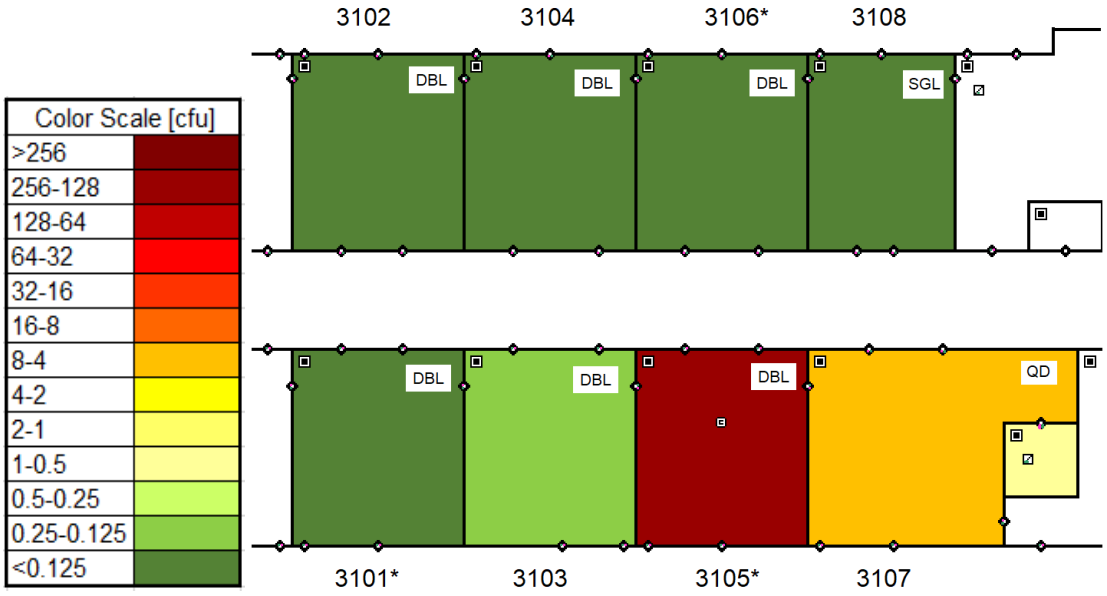

Figure 20: Simulation of spread of virus in rooms surrounding source room, 3105. The colors, defined in the logarithmic scale to the left, show the concentration of virus in cfu after two days.

The third cluster, C, was least successful of the models in predicting the locations of virus-exposed individuals. The flow paths show a large net flow of air from the source room, 3105, to its neighbor, 3107, yet none of the occupants of 3107 became infected, according to lab results. 3107 had a steady state virus concentration of 7.7 cfu

based on this model. However, the rooms in which occupants acquired a lab-verified ARI, 3106 and 3101, had negligible concentrations of virus, indicating that they were not infected due to air moved by ventilation. The errors in these predictions could be attributed to either other forms of exposure, such as movement of the room occupants through the different spaces, or different ventilation patterns caused by inaccurately modeled flow rates and directions. It is also, of course, possible that the close proximity of the rooms with ARI-positive occupants at approximately the same time was coincidental, and that the occupants were exposed in a different setting and carried the virus back to their dormitory. This is possible in any of the clusters presented.

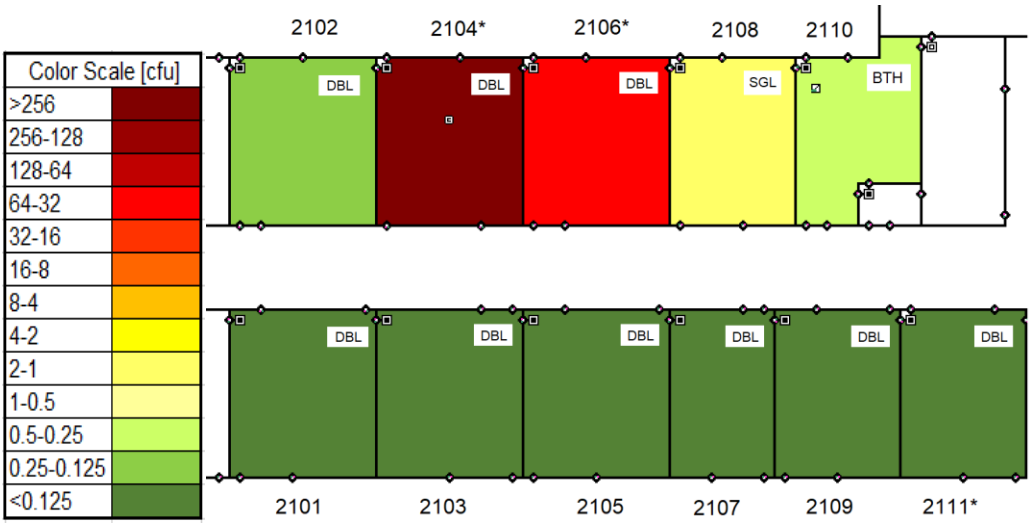

Figure 21: Simulation of spread of virus in rooms surrounding source room, 2104. The colors, defined in the logarithmic scale to the left, show the concentration of virus in cfu after two days.

Cluster D contained a source room that had outwardly directed lateral flow rates, spilling virus into its neighbors' rooms. Unlike any of the other clusters, none of the rooms across the hall were exposed to the virus, based on the modeled flow pattern illustrated in Figure 21. These results are partially consistent with the documented ARI rooms, one of which, room 2106, was adjacent to 2104 and received the largest net

flow rate, which resulted in a virus concentration of 36.2 cfu. 2106 had a net flow into its neighboring room, 2108, which received 1.3 cfu. The outmost rooms of the exposed cluster of rooms, 2110 and 2102, were exposed to 0.3 and 0.1 cfu, respectively. The anomaly is room 2111, an occupant of which became infected, but without support of direct exposure from the flow rates between rooms. As with the previous unexplained ARI rooms from clusters B and C, other factors could account for the occurrence of an ARI in this room.

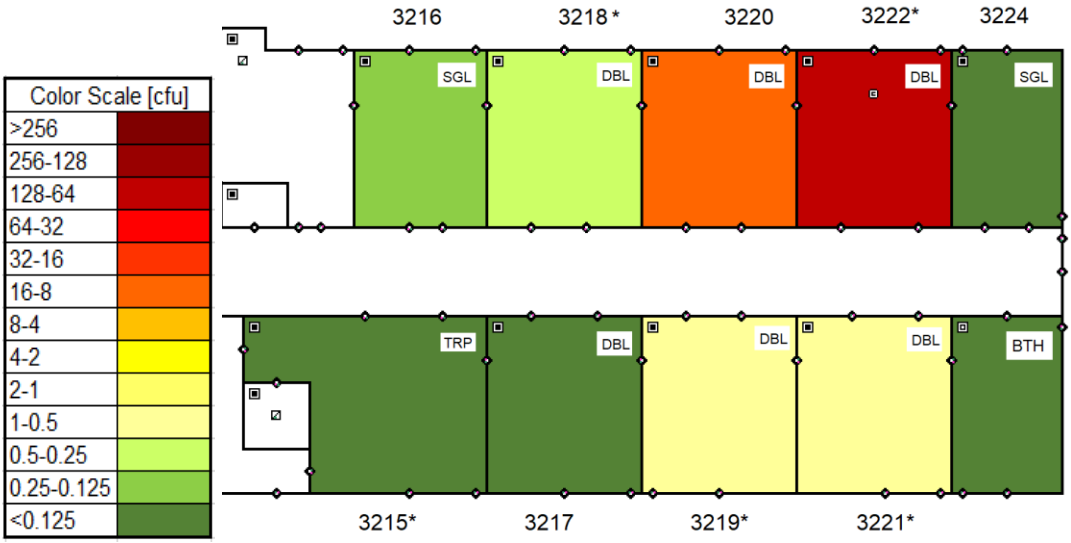

Figure 22: Simulation of spread of virus in rooms surrounding source room, 3222. The colors, defined in the logarithmic scale to the left, show the concentration of virus in cfu after two days.

Cluster E was the largest cluster, with five ARI rooms in the same length of hallway occurring in early April. Its location is notable, as the cluster, like cluster A, occurred on the end of the hall. Its ventilation model also resulted in a large percentage of ARI-positive rooms correlating to those with the highest viral exposure, with three of the four ARI-positive rooms having received significant concentration of virus from

the source room, 3222. Room 3222 had an outward net flow rate into the hallway and its neighbor to the left, 3220. This resulted in a steady state concentration of the virus in neighboring room 3220 of 9.1 cfu, and concentrations in rooms 3219 and 3221 (across the hall), which had ARI occurrences of 0.5 and 0.6 cfu respectively. While room 3220's exposure did not result in an infection, it also had the same direction of flow. Room 3218 was exposed to 0.5 cfu, possibly accounting for the occupant's ARI. The only ARI room in the cluster to receive no exposure from the source room was 3215.

A comparison of the clusters shows that success in accurately predicting the location of an ARI was more likely when the source room was on the end of a hallway. Clusters A and E demonstrate this, as the source rooms were near the end their respective hallways and had the highest steady-state concentrations of virus in same rooms that had ARI occurrences. Because the airflow from a room on the end of a hallway can only travel in one direction, rather than two, the prediction is likely to be more accurate. A source room in the middle of the hall is harder to model, and the inaccuracies demonstrated by clusters B, C, and D, show that the model calibration is not as precise towards the centers of the dormitories. Recalibration of each interior flow path with lower error permitted would improve the boundary conditions. The bulk flow prediction could also be reevaluated using computational fluid dynamics (CFD), for a different, if not necessarily better, approach.

Another reason for the success of the predictions to show great variability is because of the uncertain nature of the spread of flu virus from person to person. This cannot be accounted for by any model. Many factors play into whether or not an

individual becomes sick that are not accounted for here, such as each individual's genetic susceptibility to infection, personal hygiene, immune system, inoculation through previous exposure or the flu shot, the time spent in the contaminated environment, and others. Even if the models could accurately predict the exact flow paths and pressure differentials between each room, they can only model the possibility of exposure, not the probability of infection. Movement between the rooms, between other buildings, and time spent in each place, were not included in this model. In addition, the locations of high concentrations of the flu virus only show an increase in the probability that the occupants of that space will become sick. Individual's immune systems could prevent them from getting the flu. One more limitation comes from the inconsistency of the window/door survey responses. Only rooms that had an occupant who had a lab positive ARI test were surveyed, so it is possible that some of the rooms that were exposed to the virus but in which no one had an ARI diagnosis had kept their windows open, which would have changed the flow paths and reduced their probability of becoming infected.

3.5: Impact of Opening Windows/Doors in Student Rooms

During the spring semester, participants in the study were given a set of questions regarding their habits in opening the windows and door to their bedrooms. The window/door surveys were optional and therefore only contributed to by a small portion of the rooms tracked over the study. Despite the small sample size and the selection bias towards rooms where and when an ARI occurred, a few distinct and significant trends can be extracted from these data.

Of the 25 rooms that filled out the survey, 20 reported significant use of open windows/doors. The changes in air exchange due to opening windows and doors were calculated by redefining the orifice sizes into each room, for the number of hours that the occupants reported opening their windows and doors, in the CONTAM modeling tool and then recalculating the resulting ventilation rates. The results of these adjusted schedules are shown in Figure 23.

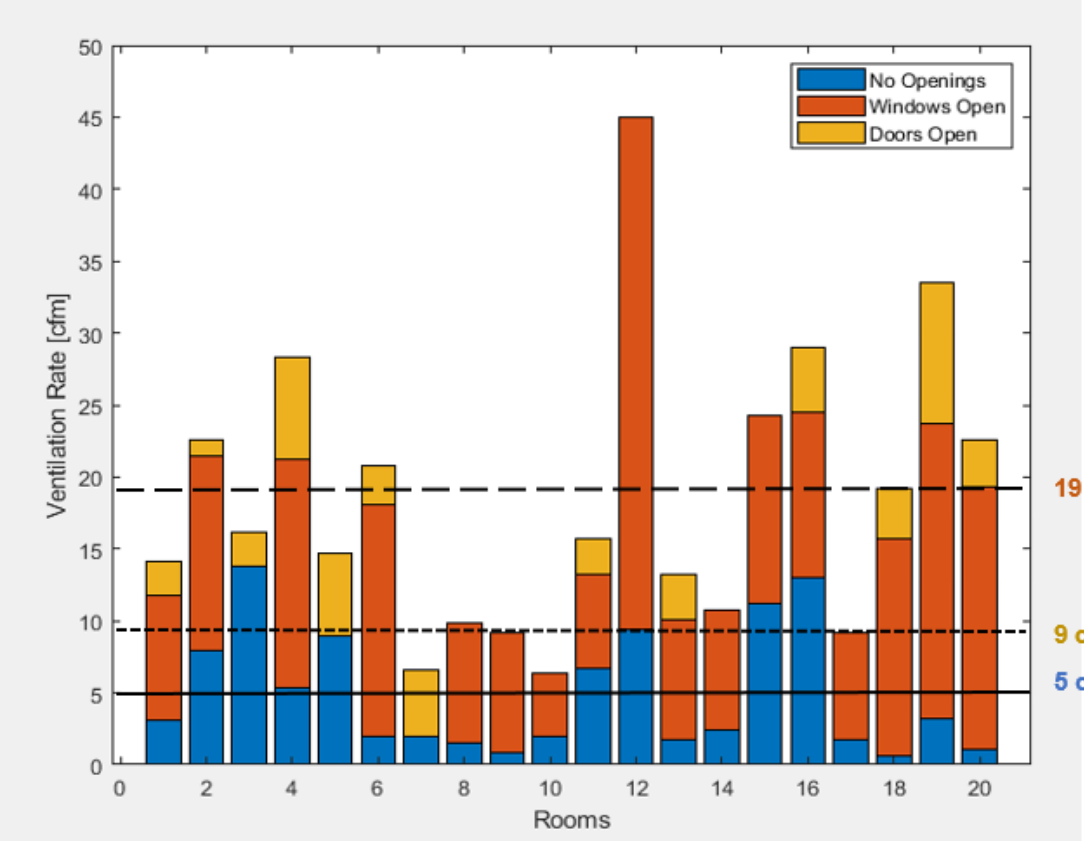

Figure 23: Change in ventilation rate due to open windows/doors as indicated by surveyed students. The average change due to having open windows was 12.9 cfm, while the change due to opening the room's door was 4.1 cfm. Opening both was predictably the most effective method of changing ventilation rates, with an average addition of 17.4 cfm of air into the room.

**Room 12 has three windows*

Each bar represents the total ventilation rate of the room. The blue section shows the original ventilation rate of the room. The red section shows the increase in

ventilation due to open windows, while the yellow section represents the increased ventilation rate as a result of the door being open. Most notable is Room 12, which has three windows as opposed to the usual one, and therefore experienced a very large increase in ventilation, 36 cfm, when they were opened.

While the ventilation rates in Figure 23 can be used to approximate the changes in ventilation for the specific rooms presented, not enough data was collected from a wide enough selection of rooms to approximate ventilation on a typical schedule of student window/door opening habits for all of the rooms in Building B. The majority of the rooms that responded had ARIs. Moreover, the days the occupants filled out the survey were usually the days of ARI detection and the days following. It is reasonable to assume that these occurrences were during times of lower-than-average ventilation, and therefore cannot predict an average student schedule of opening windows/doors, especially with the changes in outdoor temperature throughout the semester. However, the sizeable increase in ventilation due to this minimal open flow path change indicates the effectiveness of infiltration ventilation in Building B dormitory. The issue with relying on this type of ventilation to prevent ARIs is the seasonal variation in window usage. Students were less likely to have their window open in January, February, and March, likely due to the low temperature outside. As these are the months when most ARIs generally occur, it can be assumed that infiltration of fresh air through the window is a small percentage of the total ventilation of a room.

Of the five sets of cross-contamination rooms, three filled out their surveys for the days during and after ARI detection. The average time that they kept their windows and doors open during the week of infection is shown in Table 3.

Table 3: Cross contamination rooms and their self-reported window and door habits.

Room	Date of ARI	Avg time doors open [hr/day]	Avg time windows open [hr/day]
2124	2/8	4.5	0
2125	2/7	4.6	0
2127	2/13	1.3	0
3101	3/13	0	2
3105	3/9	0	0
3106	3/14	0	0.2
2104	3/14	0	8.5
2111	3/15	0	0

Notable is the trend of low window usage. With the exception of room 2104, and most likely due to the cold outside air in February and March, window use was nearly nonexistent. This would have lowered the ventilation rates throughout the rooms, increasing probability of infection. The group that became infected in February, rooms 2124, 2125, and 2127, also kept their doors open, which, though it would increase ventilation, provides a method of transportation of airborne viruses from room to room, especially if the occupants also crossed into each other's rooms during these time periods.

The group including rooms 3101, 3105, and 3106 did not keep their doors or windows open, so it is likely then that the occupants visited each other, passing the virus that then remained if the stagnant-air rooms until infecting one of the occupants.

The same situation could have caused the infections in rooms 2104 and 2111. 2104 reported keeping the windows open, but only for 5 hours on the 14th, and 12 on the 15th, after they had been infected. The lower ventilation rate on the 14th could have contributed to the inhabitant of the room falling ill, and the extended time keeping the window open the following day might have been a preventative measure by the

occupant to keep the virus from spreading further. Table 3 shows that this round of ARIs ended after only infecting three rooms, by the 16th of March, so the occupant's decision to open the window might have contributed to fewer rooms getting sick.

Cross contamination occurred almost exclusively on the 2nd, 3rd, and 4th floors. The survey shows a greater percentage of people on the lower floors (4th and below) to open doors exclusively, which encourages spread of contaminated air with the increase in ventilation. In contrast, rooms in the upper floors (5th and above), had a greater tendency to open their windows, most likely due to the greater chance of catching a breeze, as the buildings surrounding Building B are only 4 stories high.

In Figure 15, which shows the average ventilation rates in Building B, it is discernable which rooms had open windows and which opened their doors. There are several tiers in the data, but in the uppermost tier, there is a distinct upward trend in ventilation rates as the floors get higher and higher. The uppermost tier most likely represents those rooms that spent the greatest amount of time with open windows and doors, but the fact that it increases as the floor increases can mean one of two things: the higher the floor, the more time spent with windows/door open (unlikely as there are just as many or more rooms in the lower tiers who did not open their doors and windows as often), or that ventilation through the doors and windows was higher at these higher floors. While door ventilation is most likely consistent from floor to floor, the increase in ventilation through open windows increasing supports the hypothesis previously presented, that more airflow occurred through the open windows on higher levels due to less blockage from surrounding buildings and trees.

Chapter 4: Discussion

The results of this study provide a number of notable takeaways. The calculation of ventilation rates in Building A and Building B, the tracking of ARI incidence, and the self-reported habits of window/door opening all strongly support the primary conclusion that ventilation and respiratory illness are linked and that increased building ventilation can, for inhabitants that reside in the building, decrease probability of contracting an ARI from a source within that building. The results of the three study aims are summarized as follows:

- Average CO_2 concentrations in Building A, the HVB, were nearly 500 ppm lower than CO_2 concentrations in Building B, the LVB.
- Ventilation rates in Building A averaged a five times those in Building A.
- There were a sixth of the number of ARI incidences, relative to the respective dormitory populations, in Building A compared to Building B.

In addition to these results, an analysis of open flow paths revealed that opening the windows and doors in a student room increased infiltration ventilation 14 cfm on average. Opening doors alone increased the transmission of airborne viruses between neighboring rooms with poor mechanical ventilation. An analysis of the flow of a virus from a source room suggested that transmission of ARI-inducing viruses occurred at night, based on the success of closed flow path simulations in modeling accurate sick room locations, for clusters that occurred at the end of hallways.

Building B's ventilation rates ranged from barely above 0 to 14 cfm, averaging 6 cfm, which shows the large variability in infiltration ventilation, the method upon which Building B relied to receive fresh air into student rooms. Infiltration ventilation

is dependent on the opening of doors and windows as well as the construction and material components of the walls themselves. Therefore, a large component of the ventilation that these rooms received depended upon the habits of the students residing in the rooms, who chose how often and how long these were ajar. Building A's ventilation rates also differ, for the same reasons, ranging from approximately 25 to 40 cfm. As Buildings A and B had baseline ventilation rates (mechanical air supplies) of 0 and 22-29 cfm respectively, their maximum increases in ventilation were approximately 15 cfm in each building. This suggests that students who spend more time than average with open windows and doors can increase the ventilation into their room by 15 cfm, which shows a decrease in probability of obtaining an ARI. This is supported by the fact that in Building B, only one room with a ventilation rate above 10 cfm was infected during the study period. In this building, 13 rooms crossed this threshold, out of 62 total rooms.

The last step in analyzing the dormitories' ventilation rates was to compare the rates to those recommended by the American Society of Heating, Refrigeration, and Air-Conditioning Engineers (ASHRAE). ASHRAE sets a suggested ventilation rate for indoor spaces based on a number of parameters. Dormitory bedrooms were aligned with Bedroom/Living Room in Standard 62. This standard provides an equation for the ventilation rate as a function of the size of the room, as well as the number of regular occupants. The required cfm of fresh air is calculable using equation 4.1.

$$V = R_p * P + R_a * A \qquad (4.1)$$

Where V is the minimum ventilation rate, A is the zone floor area (ft^2), P is the zone population, R_p is the required outdoor airflow rate per person (cfm/person), and

R_a is the required outdoor airflow rate (cfm/ft^2). R_p and R_a are values for the minimum ventilation rates in a breathing zone taken from ASHRAE Table 6.2.2.1. The recommended air flow rate per person, R_p, was given as 5 cfm/person, and the recommended air flow rate per square foot of floor area, R_a, was given as 0.06 cfm/ft^2. In a room with openable windows, however, such as those in Centreville, ventilation is not required, as long as the window is 4% of the total floor area, and at least 5 ft^2 in area (American Society of Heating, 2013).

This study provides evidence supporting the role of fresh air in the prevention of respiratory illness. Previous literature has shown similar trends, albeit with different methodologies. The studies reviewed in Section 1.4 are of ventilation on a bus and in a single, fan-ventilated room. These two studies did similar analyses, but using CFD and the Wells Riley equation to predict the movement of particles in the single zone they each used. Both methods achieved their goals, accurately predicting flow paths and the possibility of exposure based on location within the zone. This study assumed perfect mixing within each of its many zones, and generated ventilation rates to predict the location of greatest exposure, the low ventilation building or the high ventilation building. Further analysis of smaller zone clusters tracked exposed locations using volumetric flow rate balance equation paired with a contaminant source flow equation. The results were compared to the actual locations of ARI cases. A similar goal of contamination prediction was achieved, though on a larger scale.

Chapter 5: Conclusions

The aims for this segment of a long term, multifaceted study were to collect and calibrate CO_2 concentrations for two dormitories on the University of Maryland campus - one with high ventilation and one with low, to calculate their ventilation rates, and to determine if an association exists between ventilation rates and ARI occurrences in student dormitories. The first two goals were completed using more than four months of environmental data from sensors placed in 94 bedrooms and multizone models of all rooms in the two dormitories. The overall average CO_2 concentration in Building A was 1031 ppm, while the overall average CO_2 concentration in Building B was 1512 ppm. This evidence indicates that Building B, the building with a significantly higher average concentration of CO_2, does not receive as much fresh air through ventilation as Building A. Calculation of the actual ventilation rates in the two dormitories agreed with the trends apparent in the measurement of CO_2 concentrations. The overall average ventilation rate in Building A was 30 cfm, while the overall average ventilation rate in Building B was 6 cfm.

The third aim, which hypothesized a correlation between low ventilation rates and high infection rates, was supported by the results of this study. Building A, the HVB, had only 2 ARI occurrences, while Building B, the LVB, had 30 ARI occurrences during the spring semester 2018. Alternatively, bedrooms in Building A received an average of 30 cfm of fresh air, while bedrooms in Building B received only 6 cfm of fresh air.

Two additional analyses were performed using the CONTAM models. Volunteers participating in the study were asked to fill out surveys regarding their

habits of opening their doors and windows to enable the analysis of the change in ventilation under these conditions. Based on the student surveys, a flow path schedule was created for each room, and ventilation rates were produced for the participating rooms. The simulation showed a significant increase in ventilation rates for the rooms that had significant door and window use. However, the comparatively small number of well rooms that participated in the surveys prevented there from being enough evidence to support the prediction that rooms that opened their doors and windows were less likely to become infected to draw conclusions in that regard.

The final analysis performed was to simulate the incorporation of a virus source into the models in the rooms where cross-contamination occurred between neighboring rooms in Building B, and to calculate the resulting concentrations of the virus in these neighboring rooms to determine if the simulation results predicted the actual locations of ARIs during the 2018 spring semester. The simulations showed the greatest accuracy at the ends of hallways, showing the model's limitations in calculating 2-directional flow, and suggesting that transmission may have occurred at night, when bedroom doors were closed, based on the contamination patterns.

The results of this study will be further used to perform an energy cost analysis on the dormitories. Comparing the ventilation rates in Building A to those recommended by ASHRAE standards revealed that the DOAS installed in that dormitory exceeds the necessary airflow in individual bedrooms. This unnecessary use of energy could be therefore be reduced. Along with the HVAC system, other energy loads will be analyzed in both dormitories, including lighting, electricity, and water.

From these data an energy-saving renovation could be planned to optimize the two dormitories while still prioritizing the health of the students who call them home.

Appendix A

Room Abbreviation Cheat Sheet

Dormitories

Building A/HVB

Building B/LVB

Rooms (in Building B: sgl=single room, dbl=double, trp=triple, qd=quadruple, bth=bathroom)

Cluster A: 2122(dbl), 2123(dbl), 2124*(dbl), 2125*(dbl), 2126(bth), 2127*(dbl)

Cluster B: 4220(sgl), 4221(dbl), 4222*(dbl), 4223*(dbl), 4224(dbl), 4225*(dbl)

Cluster C: 3101*(dbl), 3102(dbl), 3103(dbl), 3104(dbl), 3105*(dbl), 3106*(dbl), 3107(qd), 3108(sgl)

Cluster D: 2101(dbl), 2102(dbl), 2103(dbl), 2104*(dbl), 2105(dbl), 2106*(dbl), 2107(dbl), 2108(sgl), 2109(dbl), 2110(bth), 2111*(dbl)

Cluster E: 3215*(trp), 3216(sgl), 3217(dbl), 3218*(dbl), 3219*(dbl), 3220(dbl), 3221*(dbl), 3222*(dbl), 3223(bth), 3224(sgl)

Appendix B

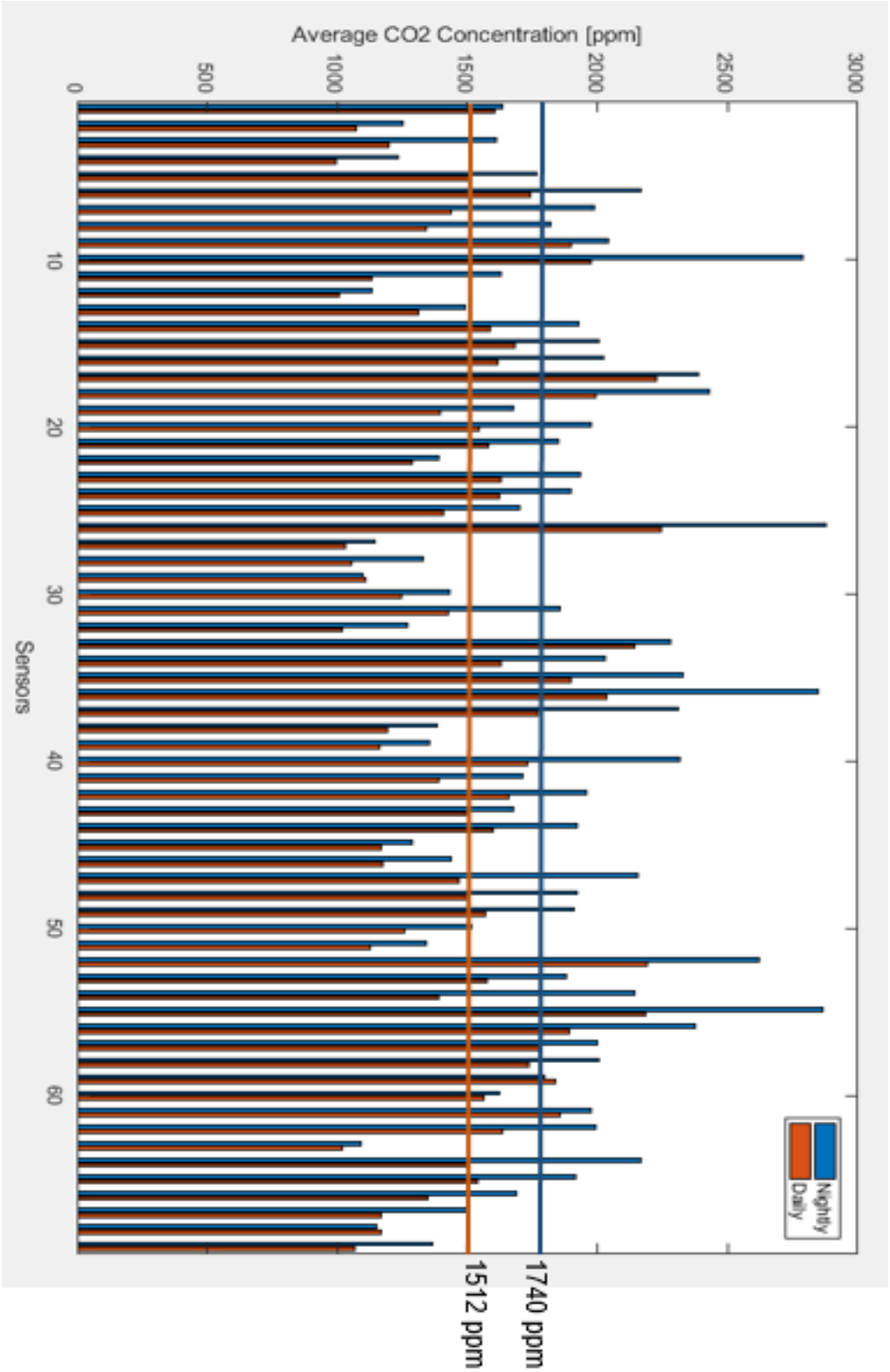

Average nightly and daily concentrations in LVB.

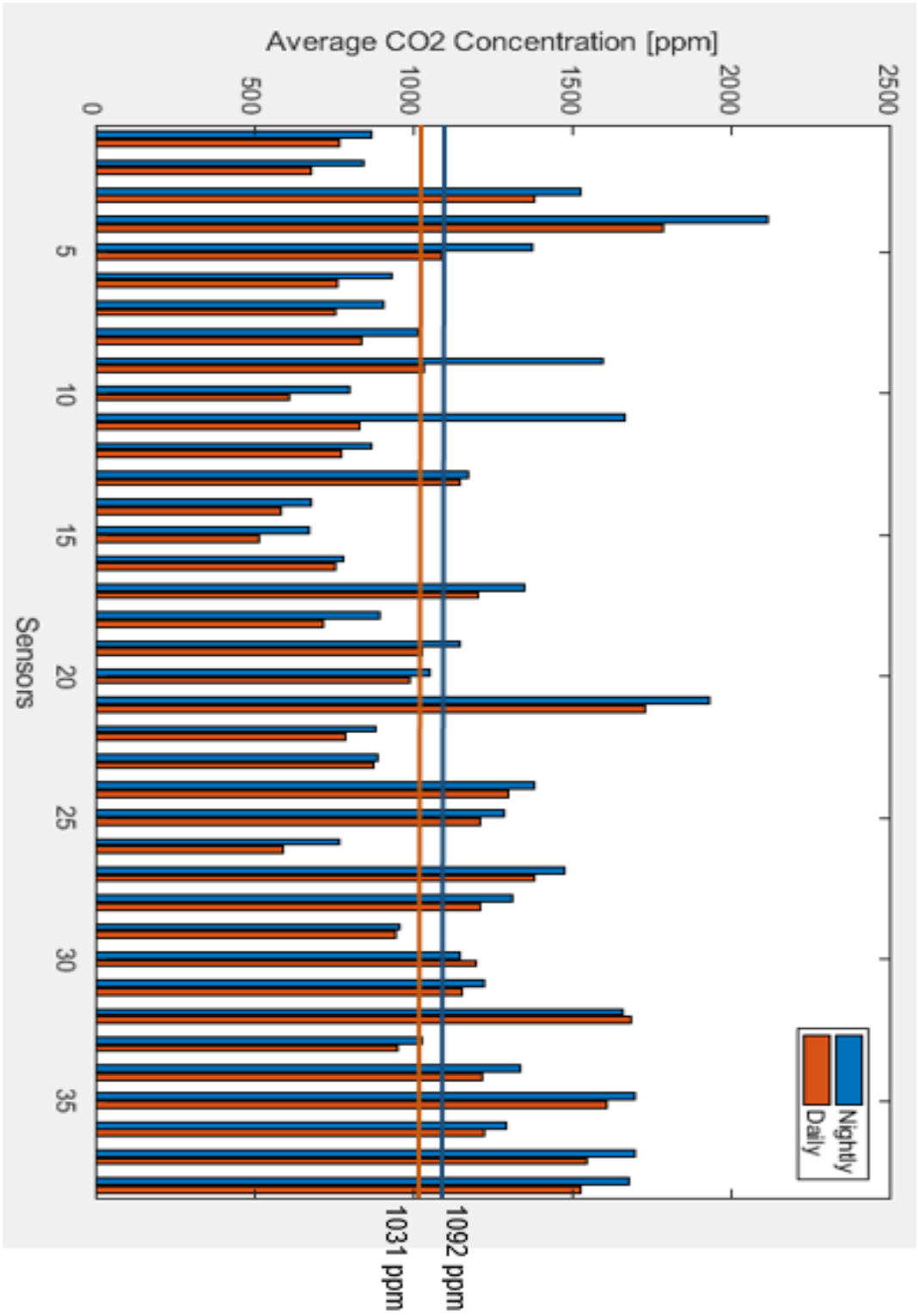

Average nightly and daily concentrations in HVB.

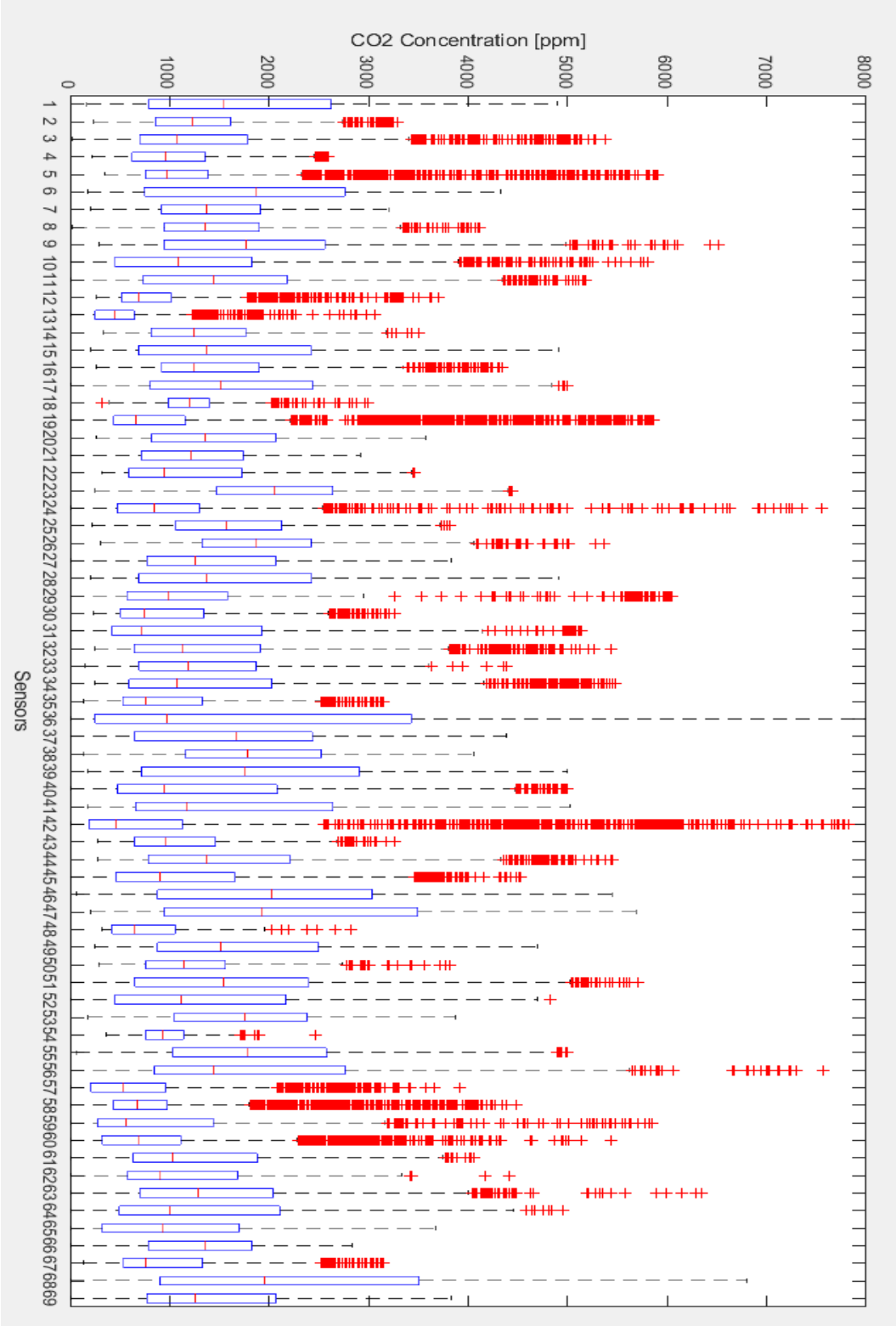

Average CO_2 concentration distribution for sensors in LVB.

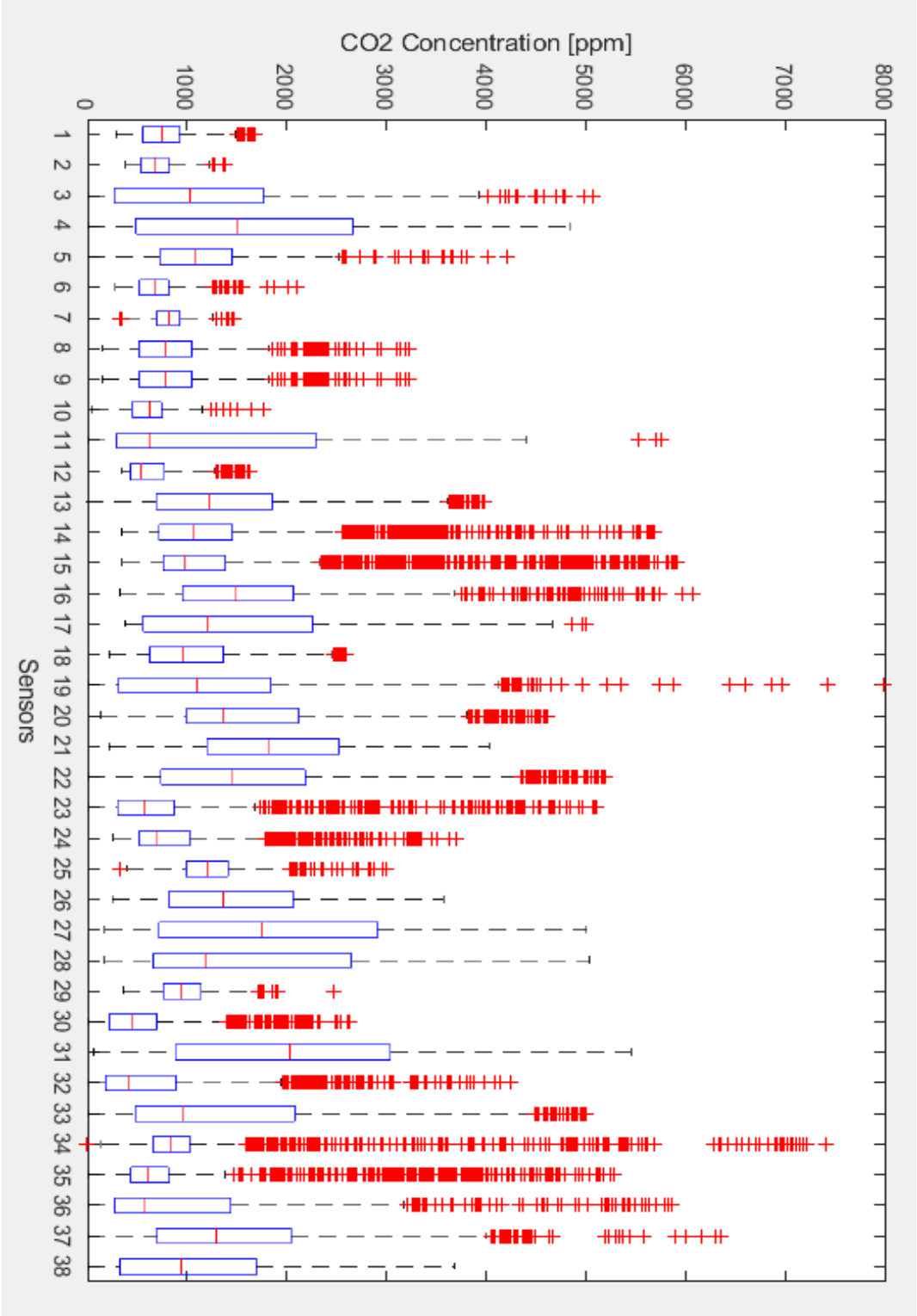

Average CO_2 concentration distribution for sensors in HVB.

Bibliography

2017-2018 Flu Season. (2018, February 12). Retrieved from Centers for Disease Control and Prevention: https://www.cdc.gov/flu/about/season/current.htm

Ali T, S. N. (2004). Detection of influenza antigen with rapid antibody-based tests after intranasal influenza vaccination (FluMist). *Clin Infect Dis, 38*(5), 760-762.

American Society of Heating, R. a.-C. (2013). *ANSI/ASHRAE Standard 62.1 Ventilation for Acceptable Indoor Air Quality.* Atlanta.

Atkinson J, C. Y.-S. (2009). Natural Ventilation for Infection Control in Health-Care Settings. *Geneva: World Health Organization*.

Balish A, G. R. (2013, July 7). Analytical detection of influenza A(H3N2)v and other A variant viruses from the USA by rapid influenza diagnostic tests. *Influenza Other Respi Viruses, 7*(4), 491-496. doi:10.1111/irv.12017

Cao, G. A. (2014). A review of the performance of different ventilation and airflow distribution systems in buildings. *Building and Environment, 73*, 171-186.

Carbon Dioxide: The National Institute for Occupational Safety and Health (NIOSH). (2011). Retrieved from cdc.gov: https://www.cdc.gov/niosh/pel88/124-38.html

CDC, C. f. (2012). Evaluation of rapid influenza diagnostic tests for influenza A (H3N2)v virus and updated case count–United States, 2012. *MMWR Morb Mortal Wkly Rep*, 619-621.

Chu, C.-M., Jong, T.-L., & Huang, Y.-W. (2005). Thermal comfort control on multi-room fan coil unit system using LEE-based fuzzy logic. *Energy Conversion and Management, 46*(9-10), 1579-1593.

Dieckmann, J., Roth, K. W., & Brodrick, a. J. (2003). Dedicated outdoor air systems. *ASHRAE journal 45*, 58.

Dols, W. S. (2016). *CONTAM User Guide and Program Documentation* (3.2 ed.). National Institute of Standards and Technology. Retrieved from http://dx.doi.org/10.6028/NIST.TN.1887

Flu Vaccine Clinic Details. (2018). Retrieved from Univerity Health Center: http://www.health.umd.edu/flu

Gao, Z. W. (2016). Potential impact of a ventilation intervention for influenza in the context of a dense indoor contact network in Hong Kong. *Science of the Total Environment*.

George, K. Z. (2007). Elevated atmospheric CO2 concentration and temperature across an urban–rural transect. *Atmospheric Environment, 41*(35), 7654-7665.

Group, T. S. (2016, September 8). *CAV vs VAV HVAC Systems*. Retrieved from https://www.theseverngroup.com/cav-vs-vav-hvac-systems/

Haghighat, E. T. (2004). Zonal Models for Indoor Air Flow - A Critical Review. *International Journal of Ventilation, 3*(2), 119-129. doi:10.1080/14733315.2004.11683908

Hall, C. B. (2017, August 1). The Spread of Influenza and Other Respiratory Viruses: Complexities and Conjectures. *Clinical Infectious Diseases, 45*(3), 353–359.

Ke, M. T., Weng, K.-L., & Chiang, C.-M. (2007). Performance evaluation of an innovative fan-coil unit: Low-temperature differential variable air volume FCU. *Energy and Buildings, 39*(6), 702-708.

Lo, L. a. (2012). Cross ventilation with small openings: Measurements in a multi-zone test building. *Building and Environment, 57*, 377-386.

Lowen, A. C. (2007). Influenza Virus Transmission Is Dependent on Relative Humidity and Temperature. *PLoS Pathog*. Retrieved from https://doi.org/10.1371/journal.ppat.0030151

Makela, E. W. (2011). *Comparison of Standard 90.1-2010 and the 2012 IECC with Respect to Commercial Buildings.* Richland. Retrieved from https://iccsafe.org/gr/Documents/IECC-Toolkit/2012IECC_ASHRAE%2090%201-10ComparisonTable.pdf

Marino, F. (2015, September 24). Project Name: Cambridge Hall Renovation. A102. Maryland: Design Collective Inc. doi:DCI Project No. 717-12-09

McDevitt, J. J., Koutrakis, P., Ferguson, S. T., Wolfson, J. M., Fabian, M. P., Martins, M., . . . Milton, a. D. (2013, January 25). Development and Performance Evaluation of an Exhaled-Breath Bioaerosol Collector for Influenza Virus. *Aerosol Science and Technology, 47*(4), 444–451.

Mortensen, D. W. (2011). Optimization of occupancy based demand controlled ventilation in residences. *International Journal of Ventilation, 10*(1), 49-60.

Nielsen, P. L.-A. (2005). Indoor Environmental Modelling: Chapter 34 in ASHRAE Handbook. *Fundamentals. American Society of Heating, Refrigerating and Air-Conditioning Engineers, Inc.*

Noakes, C. a. (2008, August 17-22). Applying the Wells-Riley equation to the risk of airborne infection in hospital environments: The importance of stochastic and proximity effects. *Indoor Air : The 11th International Conference on Indoor Air Quality and Cl*.

Novoselac, A. a. (2003). Comparison of air exchange efficiency and contaminant removal effectiveness as IAQ indices. *Transactions-American Society of Heating Refrigerating and Air Conditioning Engineers, 109 PART 2*, 339-349.

Pichurov, G., Srebric, J., Zhu, S., Vincent, R. L., Brickner, P. W., & Rudnick, S. N. (2015). A validated numerical investigation of the ceiling fan's role in the upper-room UVGI efficacy. *Build and Environ, 86* , 109-119.

Residence Halls: Cambridge Community. (2018). Retrieved from Department of Resident Life: http://reslife.umd.edu/halls/cambridge/

Residence Halls: Cambridge Community. (2018). Retrieved from Department of Resident Life: http://reslife.umd.edu/halls/cambridge/

Riley, R. (1959). Air hygiene in tuberclosis: Quantitative studies of infectivity and control in a pilot ward. *Am Rev Tuberc Pulmon Dis75, 75*(3), 420-431.

Rim, D. a. (2010). Ventilation effectiveness as an indicator of occupant exposure to particles from indoor sources. *Building and Environment, 45*(5), 1214-1224.

Sullivan, J. T. (1992, October 6). *U.S. Patent No. 5152154.*

Sun, Y. W. (2011). In China, Students in Crowded Dormitories with a Low Ventilation Rate Have More Common Colds: Evidence for Airborne Transmission. *PLOS*. doi:https://doi.org/10.1371/journal.pone.0027140

Types of Influenza Viruses. (2017, September 27). Retrieved from cdc.gov: https://www.cdc.gov/flu/about/viruses/types.htm

Wargocki, P. W. (1999). Perceived air quality, sick building syndrome (SBS) symptoms and productivity in an office with two different pollution loads. *Indoor Air, 9*(3), 165-179.

Wells, W. (1955). *Airborne Contagion and Air Hygiene.* Harvard University Press, 423.

Zhu, S., Srebric, J., Rudnick, S. N., Vincent, R. L., & Nardell, E. A. (2013). Numerical Investigation of Upper-Room UVGI Disinfection Efficacy in an Environmental Chamber with a Ceiling Fan. *Photochem Photobiol, 89*, 782-791.

Zhu, S., Srebric, J., Spengler, J. D., & Demokritou, P. (2012). An advanced numerical model for the assessment of airborne transmission of influenza in bus microenvironments. *Build and Environ, 46*, 67-75.